



Applicability of different extreme weather datasets for assessing indoor overheating risks of residential buildings in a subtropical high-density city

Sheng Liu^{a,*}, Yu-Ting Kwok^a, Kevin Lau^{b,c,d}, Edward Ng^{a,c,d}

^a School of Architecture, The Chinese University of Hong Kong, New Territories, Hong Kong

^b Institute of Future Cities, The Chinese University of Hong Kong, New Territories, Hong Kong

^c Institute of Environment, Energy and Sustainability, The Chinese University of Hong Kong, New Territories, Hong Kong

^d CUHK Jockey Club Institute of Ageing, The Chinese University of Hong Kong, New Territories, Hong Kong

ARTICLE INFO

Keywords:

Extreme weather data
Indoor overheating risk
Building thermal performance
Climate change
Residential buildings

ABSTRACT

A failure to consider extreme weather conditions in building design can lead to poor resilience and low passive survivability of buildings. Several approaches exist to construct extreme weather files for building performance assessments. Since literature comparing such extreme weather datasets is limited, this study aims to examine the applicability and limitations of the Summer Reference Year (SRY), Typical Hot Year-Event (THY-E), Typical Hot Year-Intensity (THY-I), Extreme Meteorological Year (XMY), and Typical Meteorological Year (TMY) in assessing indoor overheating risks of residential buildings, especially in a subtropical high-density living environment like Hong Kong. By comparing the simulated temperature with on-site measurements on different summer days, building physical parameters of six typical residential archetypes are calibrated in EnergyPlus. Their indoor overheating risks are then evaluated by two overheating criteria: the static extreme and adaptive thermal comfort thresholds. Results reveal that using the THY-I can generally examine the severest daytime overheating, but may fail to evaluate the maximum heat intensity of well-shaded buildings. The longest duration of daytime overheating is observed when using the THY-E, and the severest and longest nighttime overheating are found using the XMY. By contrast, using the SRY is unsuitable for assessing nighttime overheating risks. This study suggests advantages of using a combination of different extreme weather datasets, e.g., the XMY with the THYs, to assess overheating risks in high-density settings over the use of a single weather dataset. Furthermore, the building type with balconies and openable windows coated with low-e consistently demonstrates better performance than the other types.

1. Introduction

In recent years the impact of climate change on the built environment is becoming more evident due to the increasing occurrence and severity of extreme weather events, such as heatwaves, floods, and droughts [1]. These extreme events have devastating effects on the society, human health, and infrastructure systems [2]. Given that most people spend more than 90% time indoors [3] and that buildings play one of the most important roles in urban heat resistance (by providing essential shelter for residents) [4], robust assessments are required to check their resilience to more intense and frequent extreme heat events. The climate resilience and passive survivability of buildings, which refers to a building's ability to maintain safe indoor temperatures in the absence of air-conditioning (AC) [5], have stirred research interest

worldwide [6,7]. This is of particular concern to residents with limited capacity to operate an AC system, and during summertime power outages or when energy systems are overtaxed in unexpected weather conditions for which existing building systems were not designed. Particularly in the current unforeseen COVID-19 pandemic, people are spending more time indoors and the importance of diluting pollutants achieved by good natural ventilation has been brought to the public's attention [8,9]. Meanwhile, extreme weather conditions imply that a good thermal performance of naturally ventilated buildings will be more necessary in the post-pandemic period [10]. Therefore, it is imperative to examine buildings' overheating thermal performance in the face of more frequent extreme heat events.

Climatic uncertainties, for example, extremely hot events, could put buildings with poor thermal performance at risk of overheating [11]. In

* Corresponding author. School of Architecture, Lee Shau Kee Architecture Building, The Chinese University of Hong Kong, New Territories, Hong Kong.
E-mail address: sheng.liu@link.cuhk.edu.hk (S. Liu).

<https://doi.org/10.1016/j.buildenv.2021.107711>

Received 8 January 2021; Received in revised form 10 February 2021; Accepted 12 February 2021

Available online 18 February 2021

0360-1323/© 2021 Elsevier Ltd. All rights reserved.

particular, a more hostile environment caused by extremely hot events would have the most significant impact on areas with hot summers, where residential buildings are already vulnerable to the risks of overheating [12]. The majority of previous studies on overheating assessments for free-running residential buildings are found in European temperate climates, for example, the United Kingdom (UK) [13–15], the Netherlands [16,17], and Sweden [18], using available datasets of local extreme weather. Few studies [19,20] have been conducted in tropical and subtropical climates, which have more developing regions with hot summer and warm winter climates [21] and hence populations in this regions would be particularly affected by global warming [12]. For example, in subtropical Hong Kong, some 1.49 million people (~21% of the population) are still living below the poverty line [22], and the residential stocks consist of a large number of low-income housing units. According to a survey conducted in Hong Kong on living conditions in public rental housing [23], 17% of living rooms and 22% of bedrooms do not have air-conditioners installed. Furthermore, the elderly, disabled, and chronically ill people who prefer cooling by passive means such as natural or mixed-mode ventilation [24], are significantly vulnerable, along with low-income residents who cannot afford to use AC due to peak electricity pricing [25]. Different housing types and building characteristics can mitigate or exacerbate occupants' indoor heat exposure [26], hence the thermal performance of different residential building types in Hong Kong under extremely hot weather conditions is a topic worthy of investigation.

For building performance simulation (BPS), current building designs and evaluation practices usually use the Typical Meteorological Year (TMY) [27], the Weather Year for Energy Calculations (WYEC) [28] and the Test Reference Year (TRY) [29] weather files as the input climate data. These datasets represent the average climatic conditions based on 15–30 years of historical hourly data but do not consider the uncertainties of extreme weather conditions and the future changing climate. To overcome this limitation of the typical year weather data, the Design Summer Year (DSY) was first introduced in the UK to represent near-extreme weather conditions for assessing overheating risks of natural ventilated and mixed-mode buildings in the summer months [30]. Additionally, in 2013, Watkins et al. [31] proposed an alternative approach to construct a new type Design Reference Year (DRY), the DRY is based on individual months according to monthly mean dry-bulb temperature, relative humidity, and global horizontal irradiance. However, both the DSY and DRY have been criticized for poor representativeness and inconsistency with the corresponding TRY [32]. To overcome these shortcomings, in 2015 Jentsch et al. [32] developed the Summer Reference Year (SRY) by adjusting the typical weather year, TRY, to represent a more extreme summer weather condition for BPS. As the SRY was found to incorporate the high dry-bulb temperature reasonably well, it has proved more useful than the TRY in identifying severe overheating risks. More recently, Crawley and Lawrie [33] proposed a method to develop the Extreme Meteorological Year (XMY) weather files by selecting more extreme months with the highest and lowest daily or hourly average dry-bulb temperature to represent site-specific extreme climates that buildings could experience. They reported that the XMY with hourly maximum and minimum dry-bulb temperatures could best capture the range of energy load for buildings' heating ventilation and air-conditioning systems.

However, the selection of extreme situations is generally based on outdoor meteorological variables for these datasets. To account for indoor extreme events, Guo et al. [34] developed a method to construct Typical Hot Years (THYs; e.g., the Typical Hot Years-Events (THY-E) and the Typical Hot Years-Intensity (THY-I)), for BPS using simulated indoor data. The THYs weather files are defined based on the simulated indoor heat event intensity and are more focused on building performance during extreme heat events. Apart from these widely used extreme weather datasets, there are still other newly developed weather datasets that consider untypical [35] and future extreme weather conditions [36, 37]. The constructing methods of the aforementioned widely used

extreme weather datasets has been summarized in Table 1.

Above all, it can be seen that with regard to the definition of extreme conditions and the methodology to generate the dataset differ for each type of weather data, there is no consensus on which weather dataset is more appropriate and robust for assessing indoor overheating risks of residential buildings, especially in a subtropical high-density city. Although some studies [33,38] have discussed the impact of one single extreme climatic condition on the indoor thermal environment or building energy demand, there is a lack of comparative work examining the applicability and limitations of various extreme weather datasets for assessing the overheating risks of residential buildings in subtropical climates. Therefore, to fill this knowledge gap, this study is one of the first to compare the most popular extreme weather datasets, namely the THY-E, THY-I, SRY, and XMY, with the TMY for indoor overheating risk, providing insight into which extreme weather datasets can fully represent the extreme weather boundaries for assessing overheating risks of different residential building types in a subtropical high-density living environment. The results will inform architects and building engineers in other similar subtropical cities on the selection of the most appropriate extreme weather dataset for robust building assessment with various purposes. As for local interest, the results presented here will be helpful in understanding the difference of climate resilience and passive survivability between typical Hong Kong residential building types and in the formulation of action plans for designing more resilient buildings to combat the effects of climate change.

This paper is structured as follows. The methods and datasets for development of extreme weather datasets, selecting typical residential building types in Hong Kong, field measurement for building simulation calibration, and indoor overheating assessment criteria are described in Section 2. Section 3 presents the results of overheating risks using the defined static and adaptive overheating thresholds in different residential building types in Hong Kong. This is followed by a discussion on the applicability and limitations of different weather dataset and performance comparison between different residential building types in Section 4. The major findings are concluded in Section 5.

2. Methods and datasets

In this section, the methods and datasets which are used in this study are discussed as following: (1) Different extreme weather datasets were first constructed in Hong Kong based on the recorded multiple-years weather data, (2) Then, six typical high-density residential building types were selected as residential building “archetypes” in Hong Kong,

Table 1
Summary of constructing methods of different weather datasets involving extreme weather conditions.

Weather dataset	Constructing methods	Reference
DSY	The third hottest daily mean dry-bulb temperature in summer in a 20 years dataset.	[30]
DRY	Select the year according to the combined ranks of 10 years of data on either side of the 87.5 percentile year of dry bulb temperature, relative humidity and global horizontal irradiance data sequence based on 3,000 synthetic weather years produced by the UKCP09 projections.	[31]
SRY	Adjust the typical weather year TRY by employing regression equations for dry-bulb temperature, global horizontal radiation, wet-bulb and wind speed.	[32]
XMY	Combine months with highest daily or hourly average dry-bulb temperature.	[33]
THY-I	Select the year with the highest annual total heat event intensity based on the simulated indoor dry-bulb temperature.	[34]
THY-E	Select the year with the maximum event intensity and duration based on the simulated indoor dry-bulb temperature.	[34]

(3) The outdoor and indoor thermal environment of typical building types had been simultaneously measured for calibration, (4) Temperature in living room and bedroom were measured to calibrate each building simulation model in BPS tool, (5) Indoor overheating criteria for naturally ventilated buildings were finally defined for assessing building overheating: the local static extreme thresholds and adaptive thresholds provided by Technical Memorandum 52 [39]. Fig. 1 shows the methodology framework for this study.

2.1. Constructing extreme weather data

To represent different extreme weather conditions, four widely used weather datasets generated by different methods, namely the THY-E, THY-I, SRY, and XMY, were used as the different extreme weather conditions to compare with the typical year, the TMY. Based on weather data from 1979 to 2003, the existing TMY weather data in Hong Kong was constructed using the Finkelstein-Schafer statistical method [27]. In our study, to consider the more recent climate changes, key meteorological variables for building performance evaluation, including dry-bulb and wet-bulb temperature, relative humidity, direct and diffuse solar radiation, and wind speed and direction were acquired from the Hong Kong Observatory (HKO) based on the hourly weather datasets from 1993 to 2014. The HKO Headquarter’s weather station is a representative ground-level urban station in Tsim Sha Tsui, Hong Kong [40]. As extreme weather conditions usually occur in the extended summer months of Hong Kong, the construction process of extreme weather datasets was only applied from April to September.

2.1.1. Summer Reference Year (SRY)

To represent a more extreme weather conditions, the SRY was obtained by employing polynomial regression and adjusting the typical

meteorological TRY. The adjusted values for dry-bulb temperature were determined by fitting a polynomial regression between the TRY and a candidate year which is at the 90th percentile [32]. A similar adjustment method was adopted for the wet-bulb temperature and wind speed but with an additional scaling factor. The chosen approach for solar radiation was based on the 95th percentile of daily global horizontal radiation sum. Therefore, the extreme dry-bulb temperature and high solar radiation conditions were both included in the SRY generation. The detailed generation process of the SRY in Hong Kong are documented in an earlier study by authors [41].

2.1.2. Extreme Meteorological Years (XMYs)

The XMYs aim to select more extreme months than the TMY. Following the methodology developed by Crawley and Lawrie [33], we first calculated the daily maximum, minimum, and average values for each month from 1993 to 2014, and then selected months with the highest daily maximum dry-bulb temperature as the extreme “daily” months. To compare with the extreme “daily” months, the months with highest hourly average value of dry-bulb temperature were selected as the extreme “hourly” months. As the combination of extreme “hourly” months with the highest hourly mean dry-bulb temperature consistently had the higher overheating risks for all building types than the extreme “daily” months, a combination of 12 extreme “hourly” months was finally selected as the XMY year for subsequent analyses.

2.1.3. Typical Hot Years (THYs)

THYs are proposed as the weather conditions with the most extreme events but with a focus on the indoor thermal environment. Based on the different definitions of extreme conditions, three kinds of extreme weather data in summer were named as the THY-I, THY-E, and the Typical Hot Year-Night (THY-N). THY-I is the year with the highest

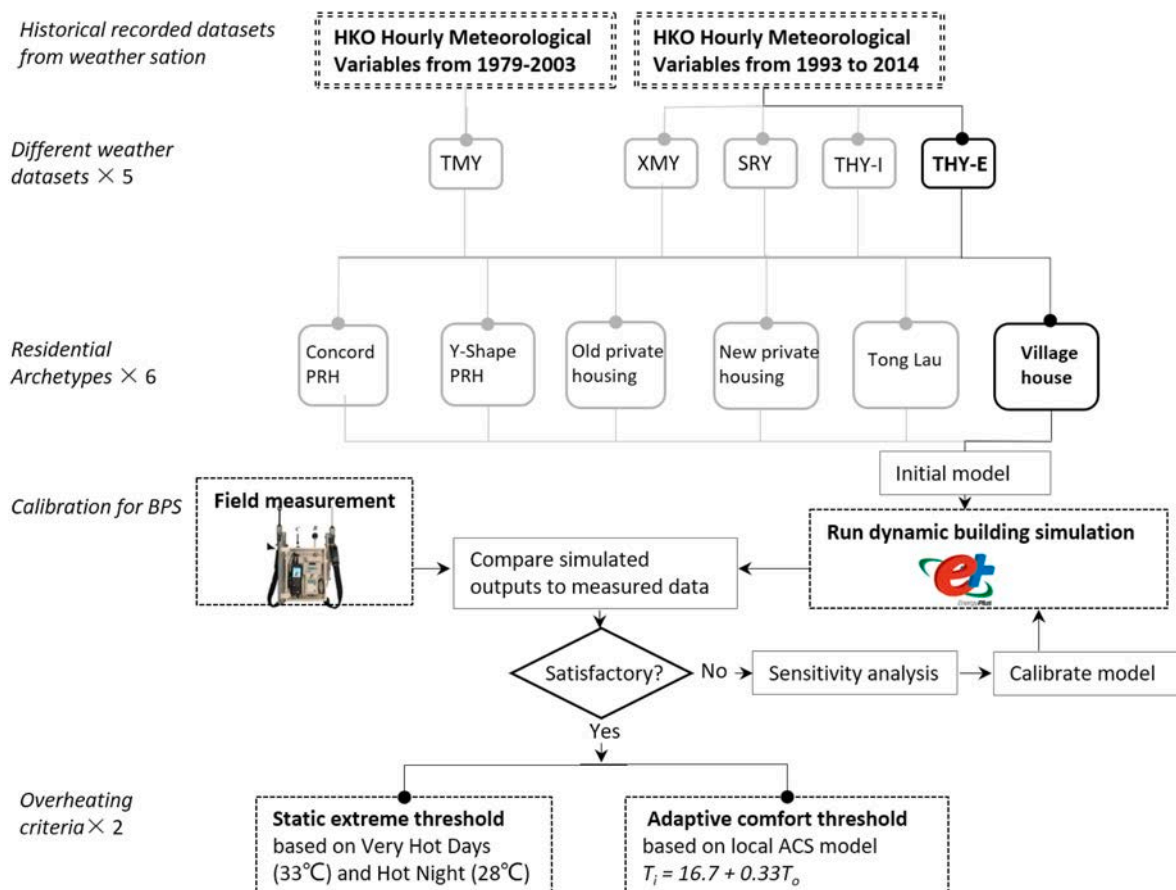


Fig. 1. Methodology framework for this study. Simulation of village house, using THY-E weather file is highlighted as an example.

annual total heat event intensity (HI) based on the simulated indoor dry-bulb temperature. Following the methodology developed by Guo et al. [42], the HI is the sum of the degree hours when the temperature is over the threshold, calculated using Eq:

$$HI = \sum_{T_{hr} - T_l > 0} (T_{hr} - T_l) \quad (1)$$

where T_{hr} is the hourly air temperature and T_l is the threshold of the accepted temperature. Here, 32.8 °C was set as T_l according to the threshold of very hot days (VHDs) in Hong Kong and the 95th percentiles of long-term temperature data, an approach adopted for defining heat-waves and assessing heat-related mortality [43,44]. Additionally, the THY-N stands for the year with the highest number of hot night (HNs). According to HKO, HNs in Hong Kong are defined as those with a daily minimum temperature above 28 °C [45]. Taking the most predominant public housing buildings and the validated building model as the reference building type [46], the year of 2014 was selected as the THY-N and THY-I simultaneously, based on the above two indicators, VHDs and HNs. Hence, only the THY-I was selected as representative for further study.

To represent the most serious extreme heat event, the year with the maximum event intensity and duration is defined as the THY-E. The weighted sum (S) of normalized values of two indices, maximum of event intensity (M) and the event duration (L), were calculated for each year:

$$S = w_M \frac{M - M_{min}}{M_{max} - M_{min}} + w_L \frac{L - L_{min}}{L_{max} - L_{min}} \quad (2)$$

where M_{max} , M_{min} , L_{max} , and L_{min} are the maximum and minimum of M and L , respectively; w_M and w_L are the weights of M and L , both values are set as 0.5 as suggested by reference [42]. The year with the highest S was selected as the THY-E.

After developing the above extreme weather datasets, the boxplots of outdoor daytime (07h00–18h00) and nighttime (19h00–06h00) temperatures above the T_l thresholds for different weather datasets are presented in Fig. 2. The comparison of other meteorological variables between different weather datasets is plotted in Fig. A1. The HI of different weather datasets for daytime and nighttime is also calculated in Table 2.

2.2. Typical high-density residential archetypes in subtropical Hong Kong

More densely populated cities and high-density buildings have been built to accommodate the rapid increases of urban population density, especially in subtropical and tropical high-density cities such as Hong

Table 2

The heat event intensity of different weather datasets for daytime and nighttime.

Weather dataset	TMY	XMY	SRY	THY-I	THY-E
HI in Daytime	0	28.7	33.7	39.3	24.2
HI in Nighttime	633.9	1479.96	889.6	1386.1	803.6

Kong. Because of the limited land area, most high-density buildings are the multi-unit and single-aspect blocks. Since the residential building stocks are heterogeneous and have a wide range of building characteristics at city scale, this study conceptually demonstrates the heterogeneous high-density residential buildings by selecting commonly found building types in Hong Kong. The building “archetype” is a widely used approach to define a set of reference buildings with the representative building characteristics specified for each building category [47]. According to the guideline of the Energy Efficiency Office of the Electrical and Mechanical Services Department in Hong Kong, it is recommended to benchmark the energy consumption indices of residential buildings in Hong Kong using the following principal groups: public rental housing (PRH), private housing, and individual houses [48]. As all PRH buildings are administered and uniformly designed by the Housing Authority and the existing number of PRH flats accommodate almost half the population [49], the predominant and latest cruciform Concord PRH buildings (after 2000s) and the Y-shape Trident PRH buildings (after 1980s), which are found in around 70% of all new PRH estates built after 1980s and will continue to be built across the city by the government in the future [50,51], were selected as the representative PRH archetypes in this study. Private housing buildings can be generally divided into the old tenement house style, often referred to as “Tong Lau” (before 1970s), old private housing (from 1970s to 2000s), new private housing (from 2000s), and village houses (the common individual building type in suburban areas) based on previous categorization studies of building archetypes in Hong Kong [52,53]. Apart from the PRH buildings, old private housing, new private housing, and Tong Lau account for 13.4%, 12.7%, and 5% of the city-scale residential stocks based on habitable floor area [53]. The built form typology within each residential archetype is considered rather homogeneous and different archetypes have different building characteristics related to building performance [54], for example, window-to-wall ratio (WWR), window glazing, building size and shape (i.e., floor area and floor layout), shading devices, external wall coating, etc. (see Table 3). Significant difference of anthropogenic heat flux between these residential archetypes in Hong Kong has also been identified by Schoetter et al. [55]. Set against the above considerations, these six residential archetypes are therefore selected as the typical residential archetypes. Photographs of the reference buildings selected for each archetype are presented in Fig. 3.

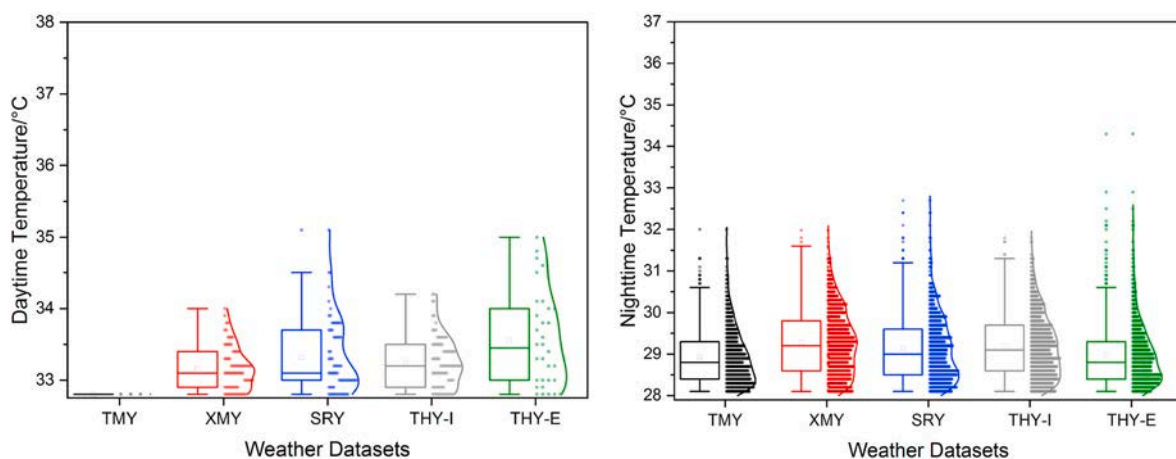


Fig. 2. Boxplots of outdoor daytime and nighttime temperature above extreme thresholds (28.0 °C for nighttime and 32.8 °C for daytime) under different weather datasets.

Table 3
Building characteristics of selected residential archetypes in Hong Kong.

Building characteristics	Concord PRH	Y-Shape Trident PRH	Old private housing	New private housing	Tong Lau	Village/Individual house
Floors:	30-45 stories	30-40 stories	8-30 stories	30-60 stories	4-8 stories	3 stories
Construction period:	After 2000s	After 1980s	1970s–2000s	After 2000s	1950s–1970s	After 1970s
Units per floor:	8 units	24 units	4–8 units	4–8 units	2–8 units	1 unit
Reference flat area (m ²):	35.3–45.9	31.9–44.3	50.8–87.7	44.5–73.7	36.0–42.5	57.0
Floor layout:	Cruciform	Y-shape	Tower-type	Tower-type	Rectangular	Rectangular
Glazing type:	Single glazing	Single glazing	Single glazing	Tinted single glazing	Single glazing	Single glazing/Tinted single glazing
Shading:	Building self-shading	Building self-shading	Bay windows/Metal overhangs	Balconies/Building self-shading	Metal overhangs/None	Balconies with living room
WWR	0.15	0.31	0.2-0.4	0.2-0.5	0.2-0.4	0.2-0.4

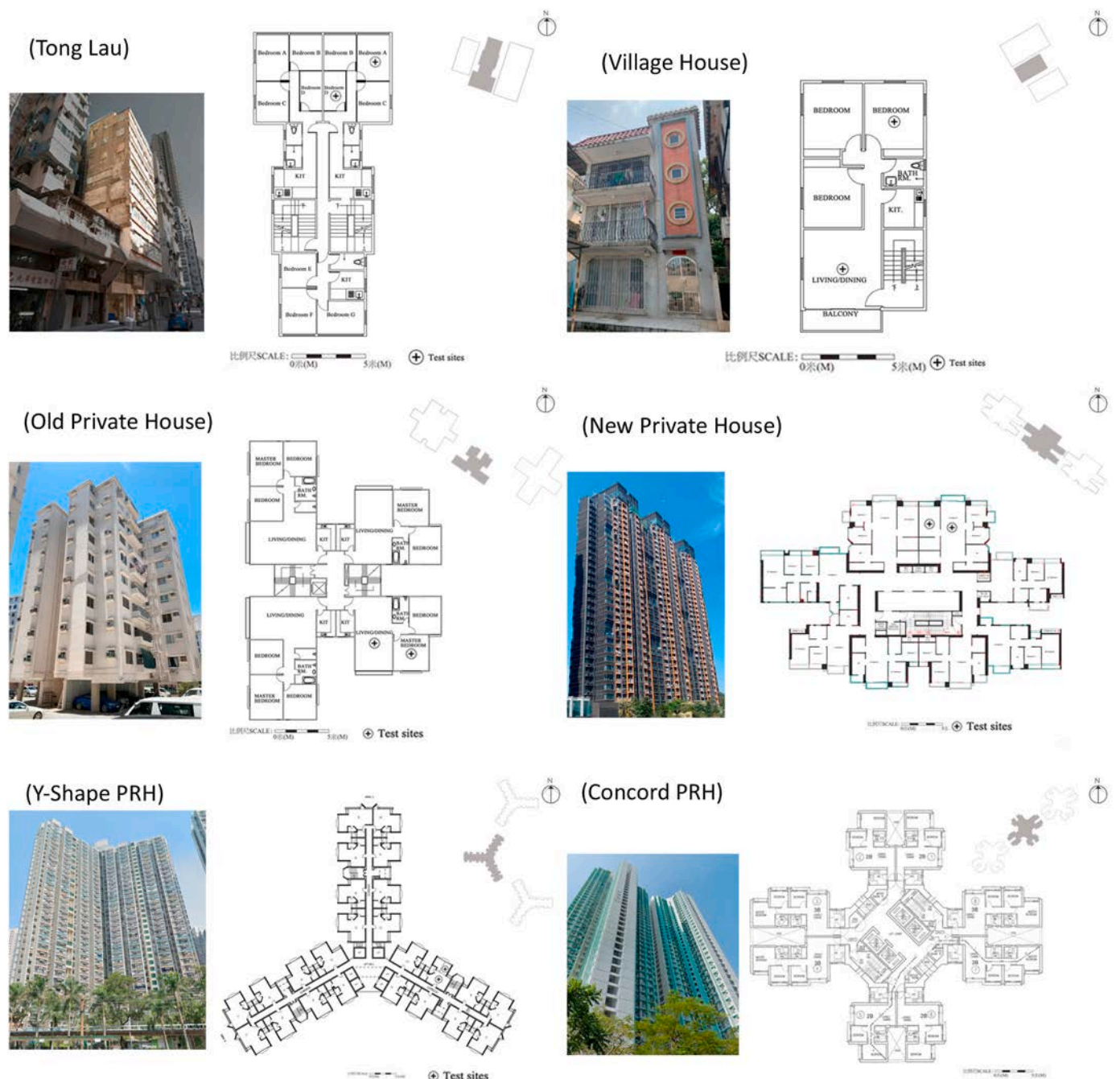


Fig. 3. The description (actual photos, floor plans and test sites) for Hong Kong residential archetypes.

2.3. On-site measurement of typical residential archetype

To calibrate the building simulation model for the selected residential archetypes, a reference building for each of those considered was selected for on-site measurement and metadata archiving. The measured flats are all located on the middle floors (i.e., neither the top nor ground floor) of the reference buildings. This is because most buildings in Hong Kong are high-rise or mid-rise buildings. Therefore, there are many more people living in the middle floors than in the top floors. The floor plan and test sites for each reference building are presented in Fig. 3. The detailed architectural drawings, building thermophysical parameters, and building construction materials of PRH buildings are well documented on the Housing Authority Department website [56] and the local green buildings scheme BEAMPlus [48], with its typical Y-shape PRH building, was included for field measurement and building model calibration. The building physical parameters of PRH buildings are listed in Table A1. Using a boxed, mounted, and calibrated Testo-480 instrument, a short-term measurement of dry-bulb temperature and relative humidity was conducted on fixed indoor test sites at a height of 1.1 m (in bedrooms and living rooms) lasting from one to two weeks in September of 2018 and May/August of 2020, to represent the typical summer indoor thermal environment of residential buildings with natural or mixed-mode ventilation. The monitoring meteorological parameters and equipment information are summarized in Table 4. The metadata of measurement conditions for different residential archetypes are also listed in Table A1. Meanwhile, the outdoor temperature, relative humidity, wind speed, wind direction, and cloud cover data at hourly intervals during the monitoring time were obtained from the HKO Headquarters while other meteorological variables including global and diffuse solar radiation were acquired from the King's Park station located at 1.2 km from the HKO Headquarters on an unobstructed point.

2.4. Calibration of the building simulation model

The building simulation models were set up with the widely used and validated building simulation tool, DesignBuilder interface, using EnergyPlus V8.5. The self-shading, external shading and surrounding buildings at sites were also constructed in the model to consider their shading effects. A calibration process was needed to identify the independent variables with uncertainty that could significantly impact the simulated outputs. As the building geometry, WWR ratio, glazing type, and shading devices can be identified from the field study, the relevant parameters were fixed as the constant input values. Whereas thermal performance, that is, the U-value of walls and floor slabs, solar absorptance of external walls, and air-infiltration of joints between envelope components were impractical to be precisely quantified due to the unknown building construction of the varied old buildings. Therefore, these parameters are sources of uncertainty, with the exception of the PRH buildings with the known thermophysical parameters and building construction materials, were taken as independent variables in the calibration process. Additionally, residents were asked to record their occupancy and window-opening schedule on an hourly basis during the on-site measurement period. The schedules for internal heat gains, window opening, and lighting were adjusted based on the recorded schedule in the calibration process. The light power density for living

Table 4
Summary of the monitoring meteorological parameters and the equipment.

Parameters	Equipment	Uncertainty and range	Measured interval
Dry Bulb Temperature (°C)	Testo-480 Digital temperature and humidity meter	±0.2 °C; -20 °C to +70 °C	1 min
Relative Humidity (%)		± (1.0% + 0.7% of measured value); 0–100%	1 min

rooms and bedrooms was set to 14 and 17 W/m² respectively according to the local code of practice, and the occupant load was set to 100 W/person [57]. As all windows and doors could be manually opened in all reference buildings, the Airflow Network model in EnergyPlus was applied to simulate the natural ventilation of residential buildings under a free-running environment.

Using outdoor weather data from meteorological stations during the measurement time as the input weather data (EnergyPlus Weather format) for the simulation of each residential archetype, the hourly simulated indoor temperature of building units was then compared with the measured hourly averaged temperature during the field measurement. To evaluate the influence of independent variables with uncertainty on the indoor air temperature, a sensitivity analysis by adjusting these uncertain building parameters was first performed. Then, a series of revisions of the uncertain variables with the sequence of importance were made to the initial model until the statistical criteria between the simulated and measured values were satisfactory, see Fig. 1. The detailed trial-and-error calibration process adopted in this study was proposed by Snyder et al. [58,59]. After the manual calibration of reference models, the modified models meeting the following American Society of Heating Refrigerating and Air-conditioning Engineer (ASHRAE) Guideline 14 [60] criteria could be assumed as the calibrated models. The goodness-of-fit of building simulation can be evaluated by the Normalized Mean Bias Error (*NMBE*) and the Coefficient of Variation of Root Square Mean Bias Error *CV(RMSE)*:

$$NMBE(\%) = \frac{\sum_{i=1}^n (t_{ip} - t_{im})}{n-1} \times \frac{1}{\bar{t}_m} \quad (3)$$

$$CV(RMSE)(\%) = \sqrt{\frac{\sum_{i=1}^n (t_{ip} - t_{im})^2}{n-1}} \times \frac{1}{\bar{t}_m} \quad (4)$$

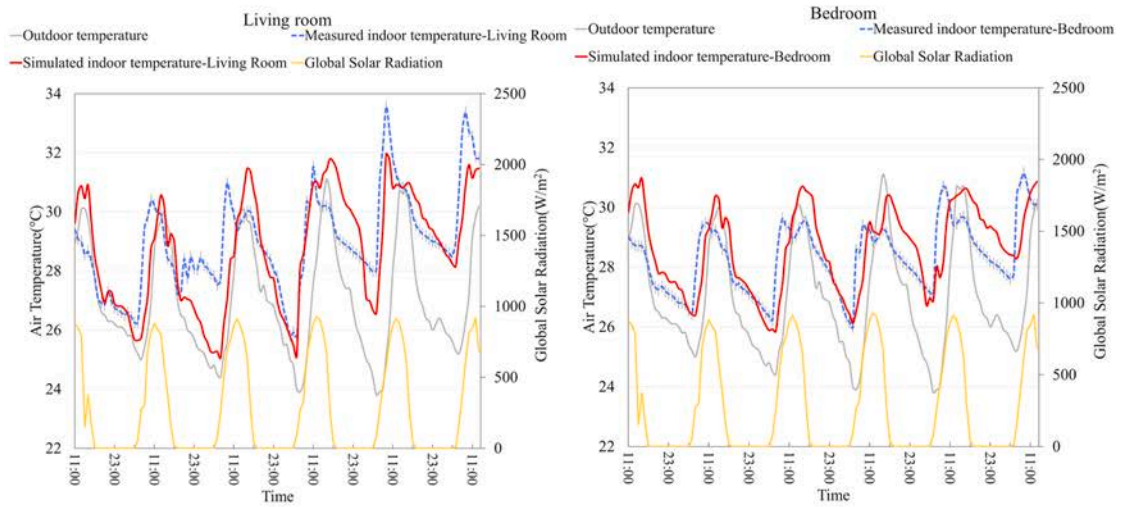
where t_{ip} is the simulated temperature, t_{im} is the measured temperature time at time interval i , \bar{t}_m is the mean value of total numbers of n measurement data. The maximum acceptable values for *NMBE* and *CV(RMSE)* are 5% and 15% for hourly data according to the ASHRAE Guideline 14.

However, it should be noted that *NMBE* only provides a value in percentage, thus knowledge of the scale of the data cannot be fully understood [61]. Besides, *CV(RMSE)* cannot normalize additive differences between datasets. Therefore, *CV(RMSE)* of one simulation period cannot be compared with other periods when they differ in an additive way [61].

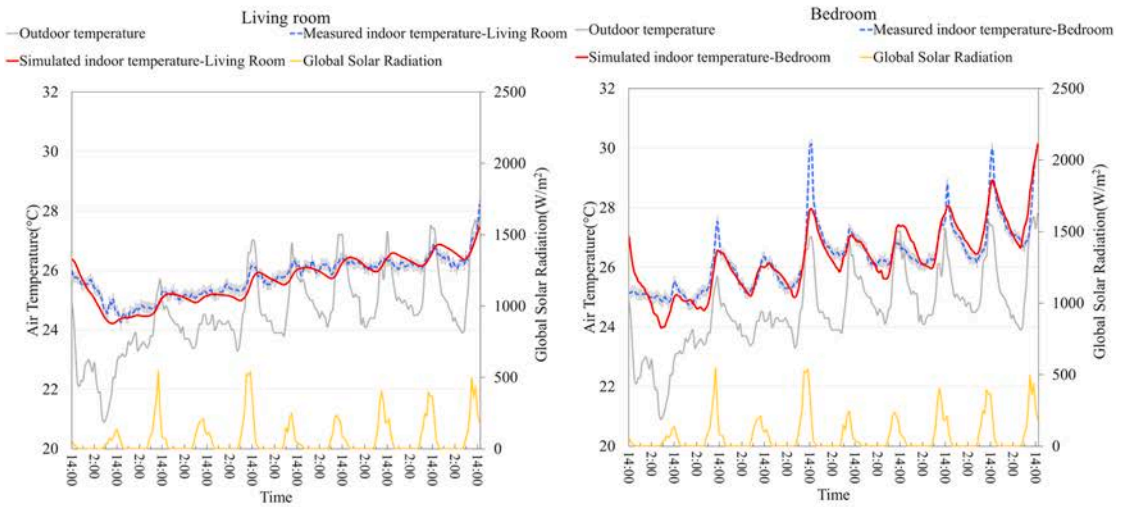
After calibrating all uncertain building parameters, *NMBE* values for bedroom and living room range from 0.17% to 1.91%, and the *CV(RMSE)* values range from 1.01% to 4.68% (Table 5). The calibrated

Table 5
NMBE and *CV(RMSE)* for each archetype and the calibrated uncertainties values.

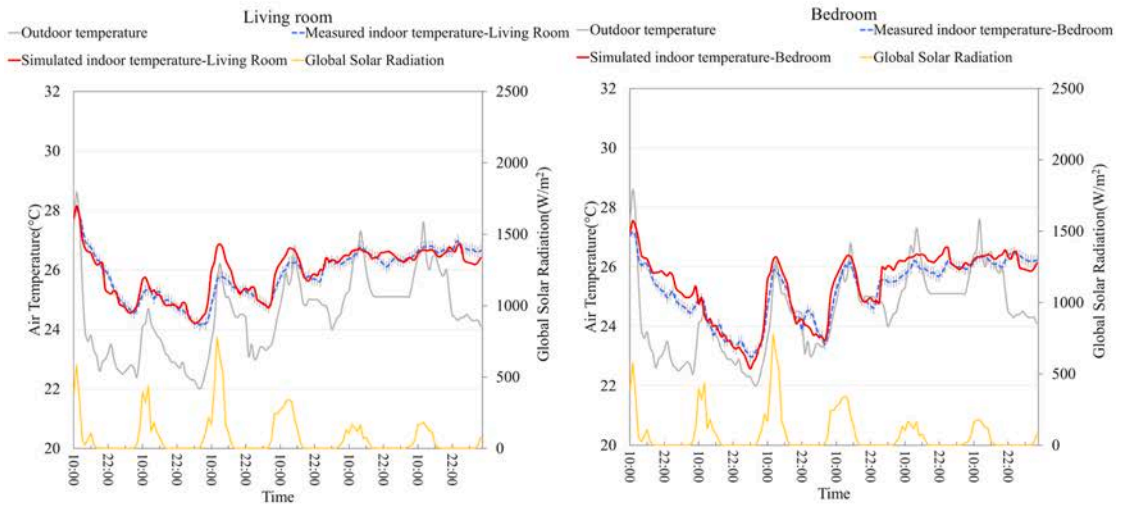
Items		<i>NMBE</i> for hourly data	<i>CV(RMSE)</i> for hourly data
Old Private House	Living room	0.86%	4.68%
	Bedroom	1.01%	3.78%
Tong Lau	Living room	0.28%	1.01%
	Bedroom	0.17%	1.76%
Village House	Living room	0.30%	1.23%
	Bedroom	0.70%	1.44%
New Private House	Living room	1.91%	2.41%
	Bedroom	0.18%	1.09%
Y-Shape Trident PRH	Living room	0.66%	1.12%
	Bedroom	0.49%	1.76%



(Old Private House)



(Tong Lau)



(Village House)

Fig. 4. Comparison of the measured and simulated indoor air temperature for living room and bedroom of different archetypes. The shaded area represents a measurement uncertainty of ± 0.2 °C.

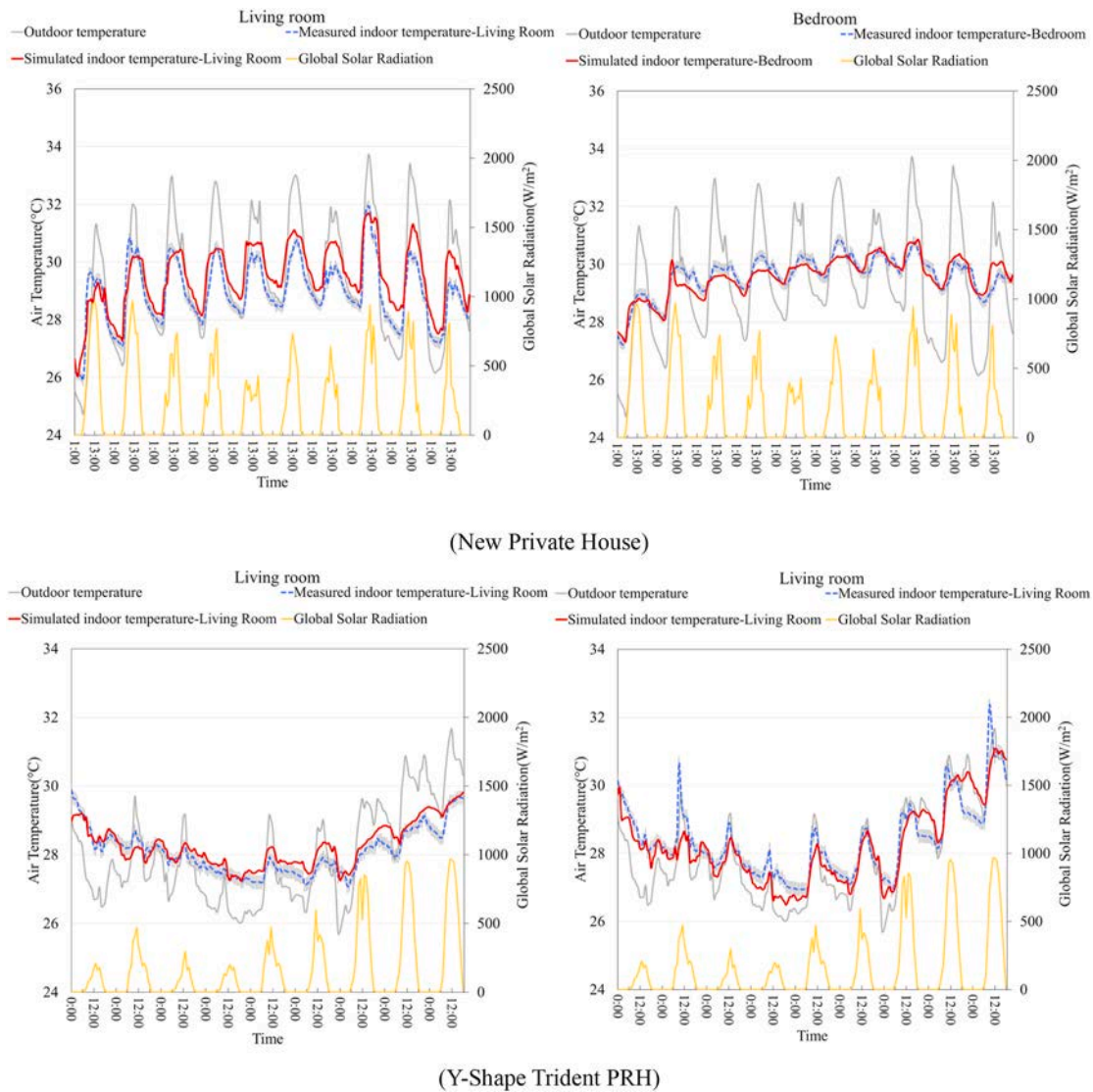


Fig. 4. (continued).

building physical parameters of the six residential archetypes are listed in Table A1. Fig. 4 compares the hourly simulated indoor temperature with the measured temperature in the living room and bedroom respectively after the calibration process. The diurnal variation of simulated temperatures is in good agreement with the measured values in the actual buildings. In terms of deviation, the main peaks in different rooms are slightly underestimated or overestimated by the simulation. This can be partly explained by the measurement errors. Since measured temperatures influenced by experimental location have the discrepancy with the simulation ones, the volume averaged values, even if the indoor measured sites are located at the center of rooms. It may also be explained by the uncertainty and fluctuation of air change rate in the measurement. Since a constant hourly air change rate was used in the building simulation, there likely are discrepancies between the averaged air change rate and instantaneously actual rate within 1 h. However, both statistic criteria of all measured archetypes met the ASHRAE Guideline 14. It means that these EnergyPlus models can be adequately credible for simulating the indoor temperature if the outdoor weather files are applicable and representative.

After calibrating the reference buildings, the standard occupancy, domestic hot water, and lighting and appliance schedules are set to the standard residential schedule profiles in Hong Kong according previous surveys in the literature [62–64], see Table A2 in Appendix. To consider

the commonly used occupant-controlled natural ventilation in Hong Kong residential buildings, the window-opening behavior is controlled by the changeover mixed-mode if the external temperature is lower than the internal one. To assess the effects of different extreme weather conditions, the newly developed extreme weather datasets in Section 2.1 are used as weather input files for building simulation for the different residential archetypes.

2.5. Indoor overheating assessment criteria

Defining a suitable thermal comfort and overheating criteria for naturally ventilated buildings is not trivial. First, three credible criteria provided by CIBSE Technical Memorandum 52 (TM52) [39] is used to identify overheating risks in naturally ventilated buildings. The room is identified as ‘overheated’ if two or more of the following criteria are met:

- **Criterion 1: Hours of Exceedance (H_e):** The number of hours during which ΔT (the difference between the actual temperature and the maximum acceptable temperature T_{max}) is equal or greater than one degree (K) shall not be more than 3% of occupied hours.
- **Criterion 2: Daily Weighted Exceedance (W_e):** The time (hours or part hour) in which the temperature exceeds T_{max} by at least 1 K is

multiplied by the number of degrees by which is exceeded. Six degree-hours is the maximum threshold in any one day.

- **Criterion 3: Upper Limit Temperature (T_{upp}):** The absolute maximum ΔT of a room should not exceed 4 K compared to the acceptable upper limitation.

Normally, the widely used adaptive comfort standard (ACS) for naturally ventilated buildings are ASHRAE 55 and the European standard EN16798 (formerly EN15251) [65]. However, the local ACS model for a specific climate, e.g., hot and humid climates, could differ markedly from the global standard originally designed for temperate climates. In areas with hot and humid climates, some literature have developed ACS model based on the ASHRAE RP-884 database [66] or large-scale thermal comfort surveys [67]. Using the ASHRAE RP-884 database, the local ACS model in Hong Kong was developed by Cheng and Ng [68]. This ACS model is selected for the indoor discomfort assessment because it introduces a function to addresses the indoor neutral air temperature (T_i) in relation to outdoor air temperature (T_o) as follows:

$$T_i = 16.7 + 0.33T_o \quad (5)$$

The acceptable temperatures set the limits of the acceptable zone and the range of acceptable temperatures are 3.5 K for 80% acceptable upper limitation and 2.5 K for 90% acceptable upper limitation. The 80% and 90% acceptable upper limitations are used for T_{max} in *Criterion 1*.

The criteria for representing the severity and quantity of heat events mainly include the duration, frequency, and magnitude of heat events [34]. As the scope of this study is to quantify overheating risks under the extreme weather conditions, two indices including overall intensity represented by HI and duration of heat events represented by L were used. In addition to the TM52 approach based on the adaptive comfort model, the static extreme event thresholds, HI and L of prolonged heat events, which are strongly associated with mortality [25] (same as Eq (1) based on the thresholds of T_b , i.e., VNs and VHDs) were adopted to assess the indoor overheating and building passive survivability under extreme weather conditions. Rather than the commonly used daily data for outdoor thermal comfort assessments, the hourly data were selected for the indoor thermal comfort assessment as it is the focus of this study.

3. Results

3.1. Overheating risks using static extreme event thresholds

According to the occupancy profile of different rooms, the occupied hours 08h00 to 23h00 and 23h00 to 07h00 were included for assessment of the overheating risks above static extreme thresholds of T_i in the living rooms and bedrooms, respectively. The HI and L of heat events for six archetypes were compared between different weather conditions (see Table 6). It can be seen that the impact of extreme weather conditions on the indoor HI varies across the different weather datasets and a considerable difference of overheating risks was observed in living rooms and bedrooms in daytime and nighttime, respectively.

Fig. 5 shows the violin plots of overheating during the occupied time of living rooms. In the daytime, overheating risks based on VHDs were evident in all the extreme weather datasets, whereas there were no overheating risks in any archetypes under the TMY condition. It is also noteworthy that daytime overheating risks were observed in most archetypes under the different extreme conditions. The exception was the New Private House where no exceedance of the extreme T_i threshold was simulated for the living room. Compared with the typical weather condition, the TMY, HI in the daytime can increase up to 26.34 for the XMY, 22.68 for the SRY, 28.75 for the THY-I, and 19.63 for the THY-E.

Table 6

The intensity (HI) and duration (L) of heat event for archetypes under different weather conditions.

Archetype	Indicator	TMY	XMY	SRY	THY-I	THY-E
New Private House	HI in daytime	0	0	0	0	0
	L in daytime	0	0	0	0	0
	HI in nighttime	534.99	1384.94	668.48	1246.63	625.91
	L in nighttime	139	222	104	221	156
Concord PRH	HI in daytime	0	26.34	22.68	28.75	18.86
	L in daytime	0	6	5	7	8
	HI in nighttime	645.46	1551.13	820.05	1403.69	815.43
	L in nighttime	105	198	103	187	116
Old Private House	HI in daytime	0	17.39	21.67	23.23	17.00
	L in daytime	0	7	6	4	8
	HI in nighttime	829.72	1836.36	1050.60	1678.82	972.74
	L in nighttime	139	222	112	212	178
Tong Lau	HI in daytime	0	3.19	2.73	0.44	2.37
	L in daytime	0	8	8	3	7
	HI in nighttime	694.40	1676.81	855.25	1530.33	900.21
	L in nighttime	105	222	103	193	163
Village House	HI in daytime	0	3.32	5.54	3.37	12.00
	L in daytime	0	5	5	4	8
	HI in nighttime	634.77	1690.78	820.68	1551.66	896.06
	L in nighttime	154	223	108	223	169
Y-Shape PRH	HI in daytime	0	18.61	21.06	22.79	19.63
	L in daytime	0	7	6	5	9
	HI in nighttime	565.50	1421.94	723.66	1254.18	710.25
	L in nighttime	67	170	100	168	115

Note: The maximum of each indicator of different archetypes are marked as bold numbers.

The maximum of daytime HI in different archetypes is normally identified when employing the THY-I where it shows a higher probability density than the SRY and XMY, except for the archetypes of Tong Lau and Village House. Additionally, the longest event of daytime L and the maximum daytime temperature generally occurred when using the THY-E for all archetypes.

Fig. 6 shows the violin plots of overheating in the occupied time of bedrooms in different archetypes. Compared with the TMY, a significant increase in nighttime HI under the weather condition of the XMY (121–164%) and the THY-I (102–144%) can be observed in the bedrooms. The indoor nighttime HI was more severe than outdoors in all weather datasets (see Table 2). Furthermore, the longest event of nighttime L and bimodal probability distribution daily oscillations of indoor air temperature were all found for the XMY. A similar bimodal probability distribution was found in the THY-I. The relative

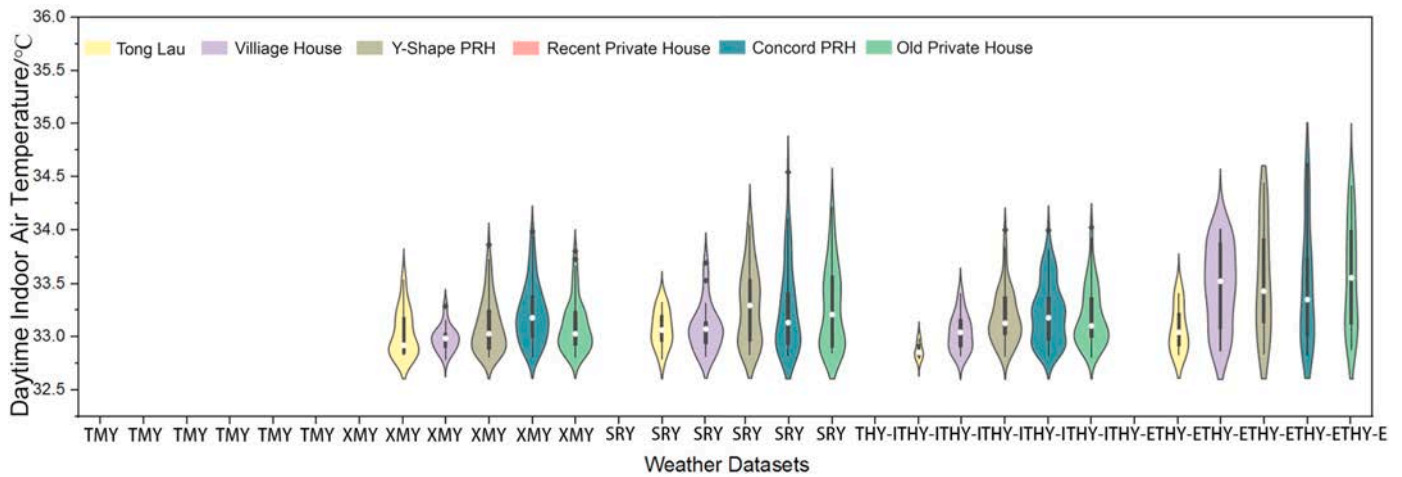


Fig. 5. Violin plots of overheating in occupied time (08h00 to 22h00) of living rooms under different extreme weather conditions. Note: the empty bar indicates no temperatures above the threshold.

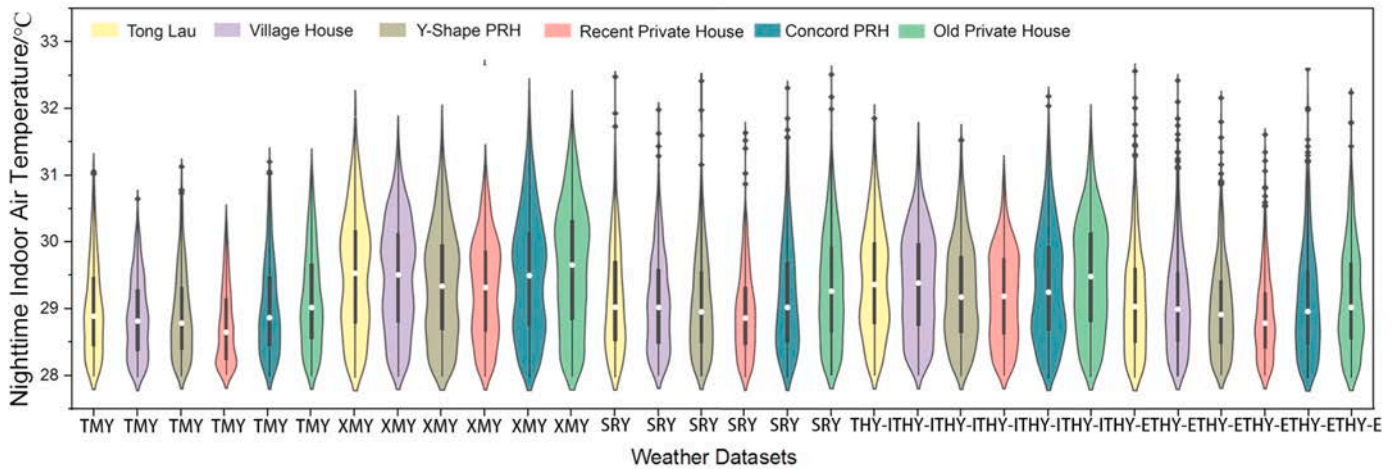


Fig. 6. Violin plots of overheating in occupied time (23h00 to 07h00) of bedrooms under different extreme weather conditions.

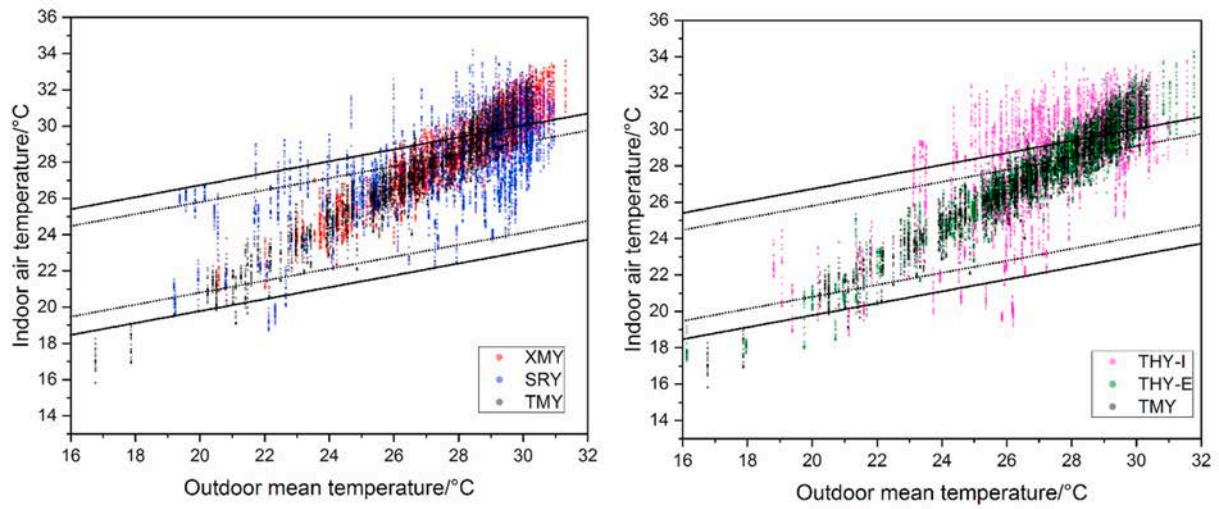
discrepancy of cumulative heat intensity and nighttime L between the THY-I and the XMY was negligible, as shown in Table 6. By contrast, slightly increased risks in terms of HI were found for the SRY and the THY-E. There was only a 23–29% increase of HI risks for the SRY, and a 17–41% increase for the THY-E, compared with the TMY. As for nighttime L , the relative increase in the THY-E varied from 9 to 72%. Meanwhile, the SRY even had a marginally decreased nighttime L (-30–2%). However, the maximum and outliers of nighttime temperature often appeared in the SRY or THY-E.

3.2. Overheating risks using the TM52 approach based on the adaptive comfort model

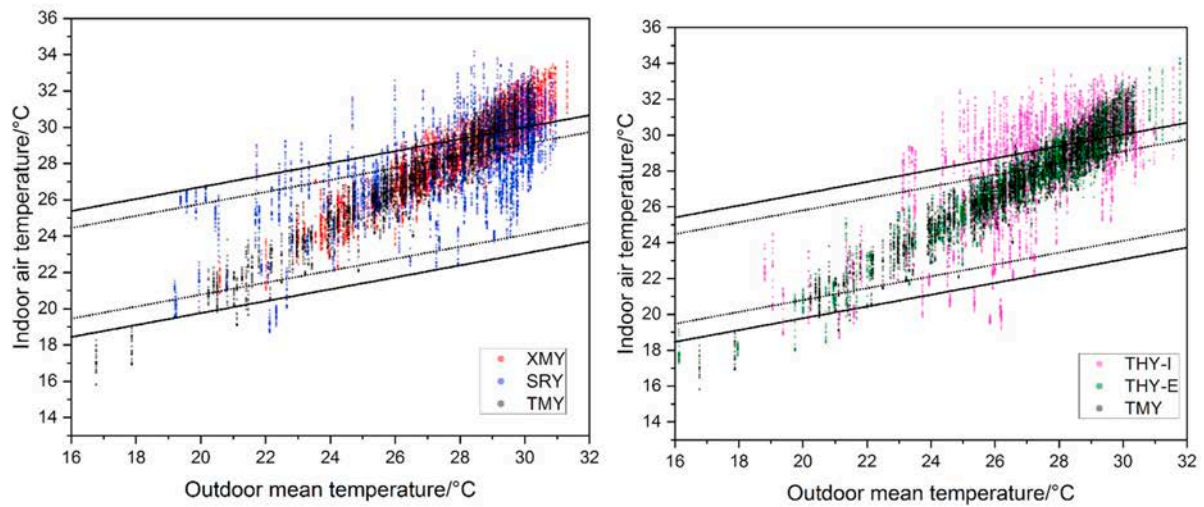
To further explore the adaptive thermal comfort of naturally ventilated or hybrid buildings under the various extreme weather conditions, Fig. 7 represents the hourly indoor air temperature versus the daily outdoor mean temperature over the entire year in different archetypes. The hourly indoor air temperature is compared with the 80% and 90% acceptable upper limitations in the local ACS model mentioned in Section 2.5. Overall, all archetypes experienced discomfort hours in all the weather conditions under consideration based on the upper limitations

of the ACS model. Moreover, most daily oscillations of indoor air temperature in the TMY were lower than 5 K during the summertime; but the daily oscillations of indoor air temperature in the same archetype were considerably amplified by the outdoor extreme weather conditions, especially the THY-I and SRY. Particularly on some days with a low outdoor mean temperature, a higher risk of indoor air temperatures was observed when using the SRY and THY-I compared to the XMY and THY-E. Additionally, the number of hours beyond the upper ACS limit was considerably varied among different archetypes, for instance, Concord PRH and New Private House, while the daily oscillations in different archetypes experienced a similar trend for the same weather type.

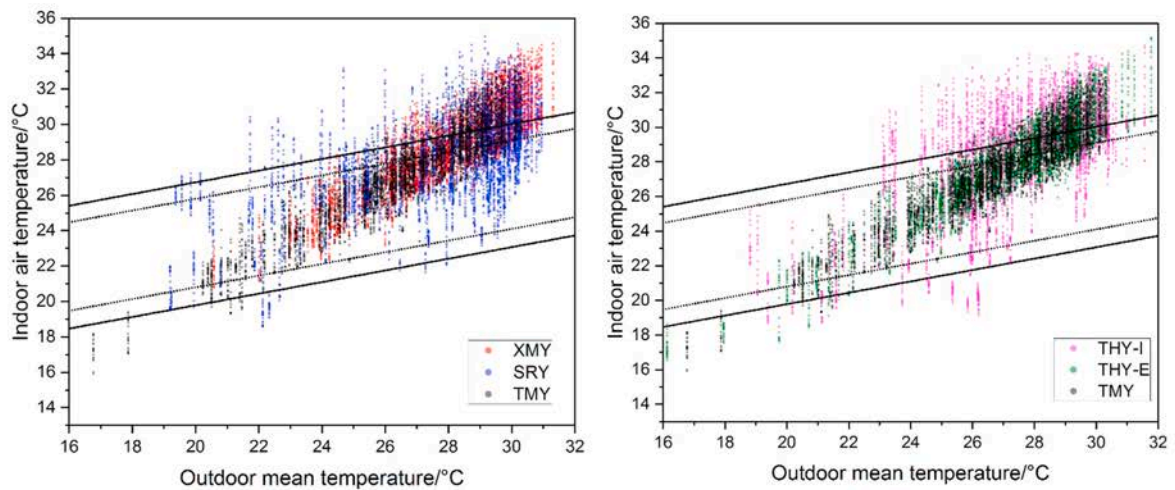
Fig. 8 shows the hours of exceedance (He) for different archetypes quantified by the ACS model under different extreme weather conditions. As the TM52 adaptive approach suggests considering the occupancy of different rooms, the occupied hours were considered separately for the living rooms (daytime) and bedrooms (nighttime). In contrast to the static thresholds in Section 3.2, the severity of overheating risks in living rooms and bedrooms based on the adaptive approach has reversed; the magnitude of He in the daytime was considerably higher than that during the nighttime. All archetypes experienced a large



(Concord PRH)



(Old Private House)



(Tong Lau)

Fig. 7. Hourly indoor air temperature versus the daily outdoor mean temperature under the different weather conditions.

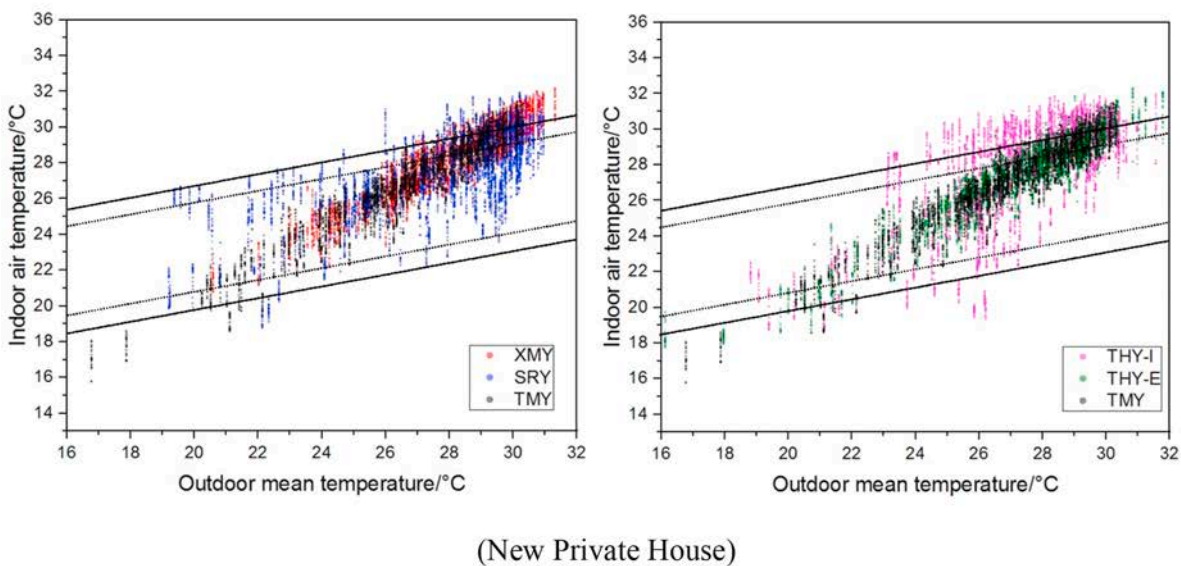
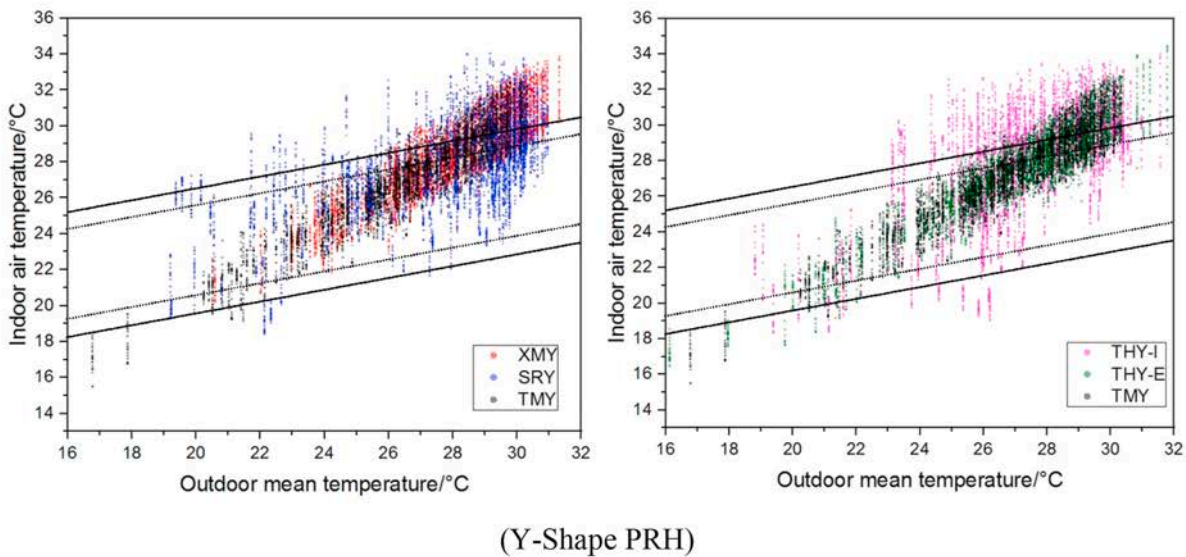
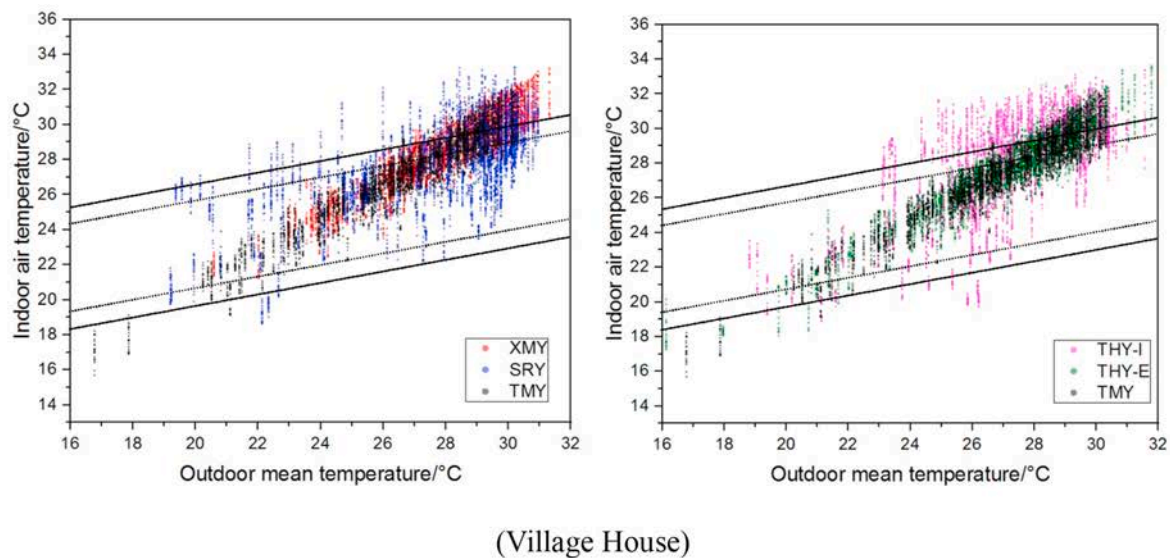
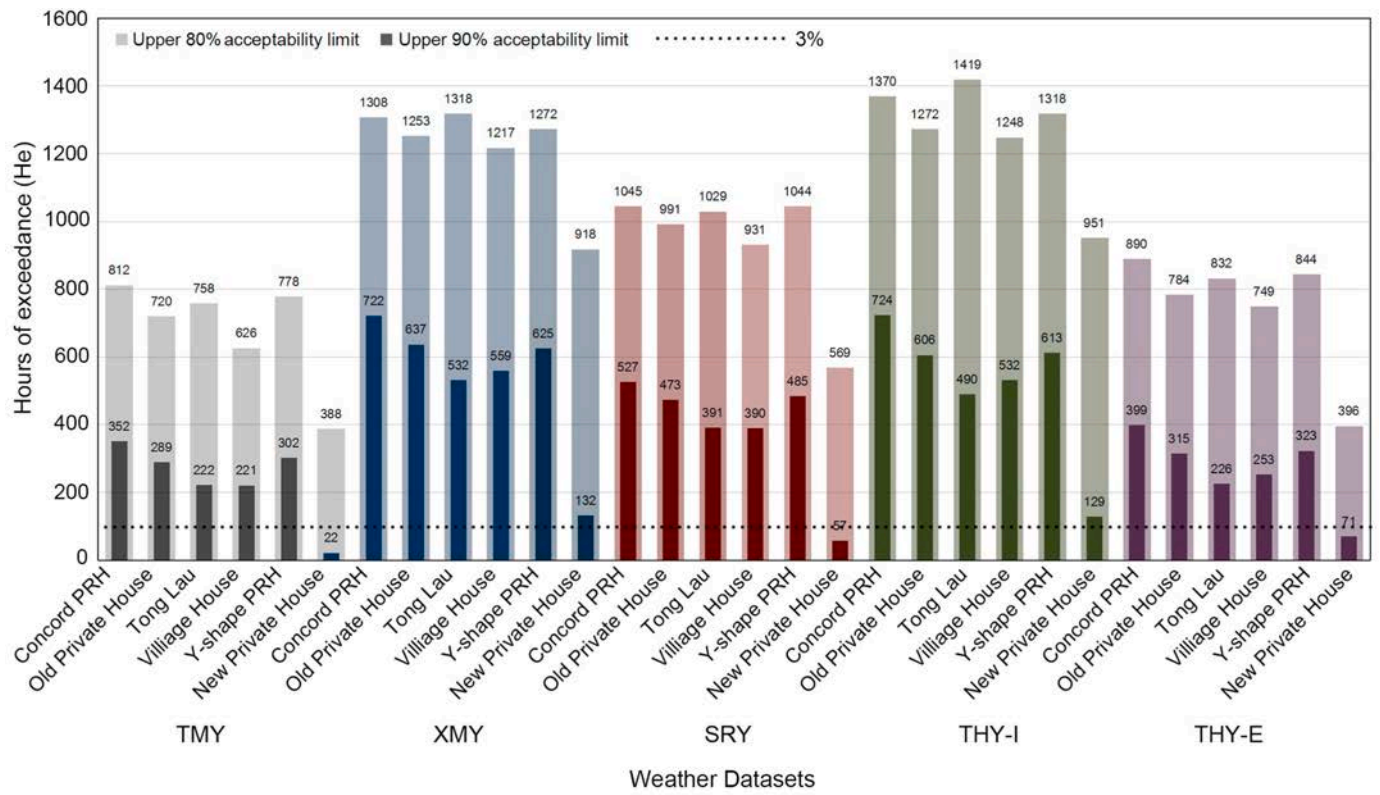
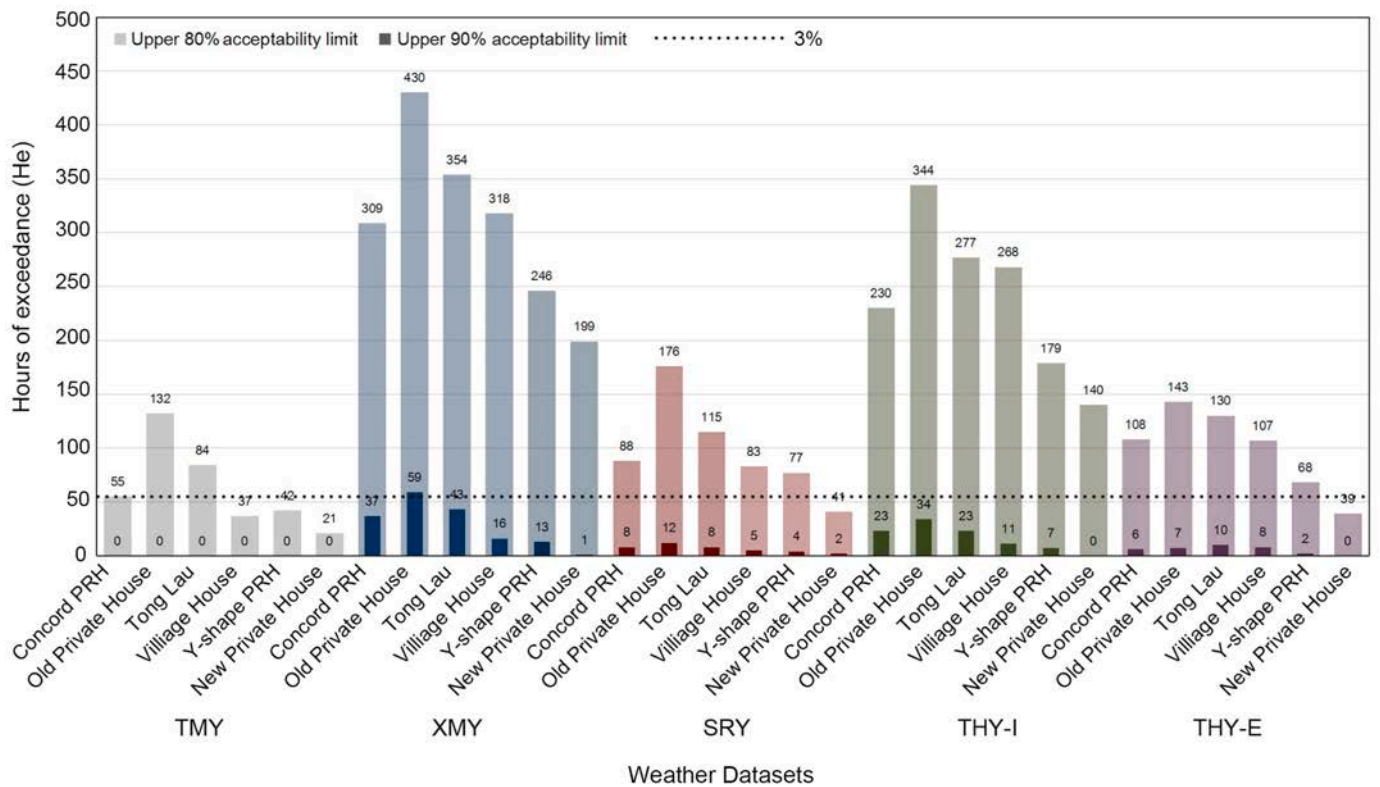


Fig. 7. (continued).



(a)



(b)

Fig. 8. The hours of exceedance (H_e) for different archetypes under different weather conditions (a) daytime and (b) nighttime.

number of He (more than 3% of the occupied time) in the daytime, while some archetypes satisfied *Criterion 1* at nighttime, for example, the Village House and Y-Shape House in the TMY, and New Private House in the TMY, SRY, and THY-E. When comparing the impact of different extreme weather datasets, the most remarkable characteristic is that He of the THY-I and XMY was significantly higher than that of the TMY, especially at night. The increase of He for the XMY and THY-I was up to 847% and 624%, respectively, taking the number of He at the 90% acceptable upper limit of the TMY as baseline. However, the number of daytime He shows an insignificant increase of 28–48% for the SRY and 2–9% for the THY-E. This pattern using the adaptive threshold is similar to that of the static thresholds. Moreover, the number of daytime He for the THY-I was larger than that for the XMY in all archetypes, while the number of nighttime He for the XMY was larger than that for the THY-I.

Fig. 9 and Fig. 10 depict the days with Weighted Exceedance (We) more than 6 and Upper Limit Temperature (T_{upp}) for all archetypes under different weather conditions. It can be seen that most archetypes fail to comply with *Criterion 2* even at the 80% acceptable upper limit, with the only exception being the New Private House which does comply with *Criterion 2*. The pattern of disparities of We between the TMY and the other extreme datasets is similar to the trend of He , although most of the disparities of We are larger than those of He . When the We was examined separately during daytime (in living rooms) and nighttime (in bedrooms), most were found in the living rooms with only a small amount at bedrooms. In the case of T_{upp} , different extreme weather datasets show one or two K higher than the TMY. However, there was no significant difference of T_{upp} between different extreme weather datasets. The daytime T_{upp} of Concord PRH, Old Private House, and Y-shape PRH failed to comply with *Criterion 3* under extreme weather conditions, whereas all archetypes complied with *Criterion 3* at nighttime.

4. Discussion

4.1. The applicability and limitations of different weather datasets

The findings in Section 3 illustrate the importance of considering the robustness of the building thermal performance against different weather boundaries. On the one hand, the results show that the most severe HI and He in the daytime for most of the modeled archetypes can be identified when using the THY-I, while the most severe nighttime HI and He can be highlighted by the XMY. On the other hand, the longest daytime L for a heat event can likely be found when using the THY-E weather dataset. However, the methods for constructing the XMYs have been challenged by some researchers [34,69], because the XMYs could tend to overestimate the overheating due to its constructing method by combining months with the highest daily or hourly mean temperature which, in reality, is unlikely for all of them to occur in the same year. It is also questionable whether combining the most extreme months is useful for finding design solutions to respond to the extreme weather conditions as this may lead to design solutions with a very long return period. To assign appropriate return periods for hot events, it is interesting to note that CIBSE Weather Files 2016 [70] proposed the new probabilistic DSY which contains a range of overheating events with different return periods. However, the effects of solar radiation and other climatic variables which could be crucial for overheating risks of heavily glazed buildings in subtropical cities have been ignored in this weather data. In this study, it is also noted that the difference of HI and He between the XMY and THY-I was not significant especially in the daytime. Which means the XMY could be a supplementary way to consider the one of most extreme conditions even if it may slightly overestimate the overheating in the nighttime. By contrast, the selection

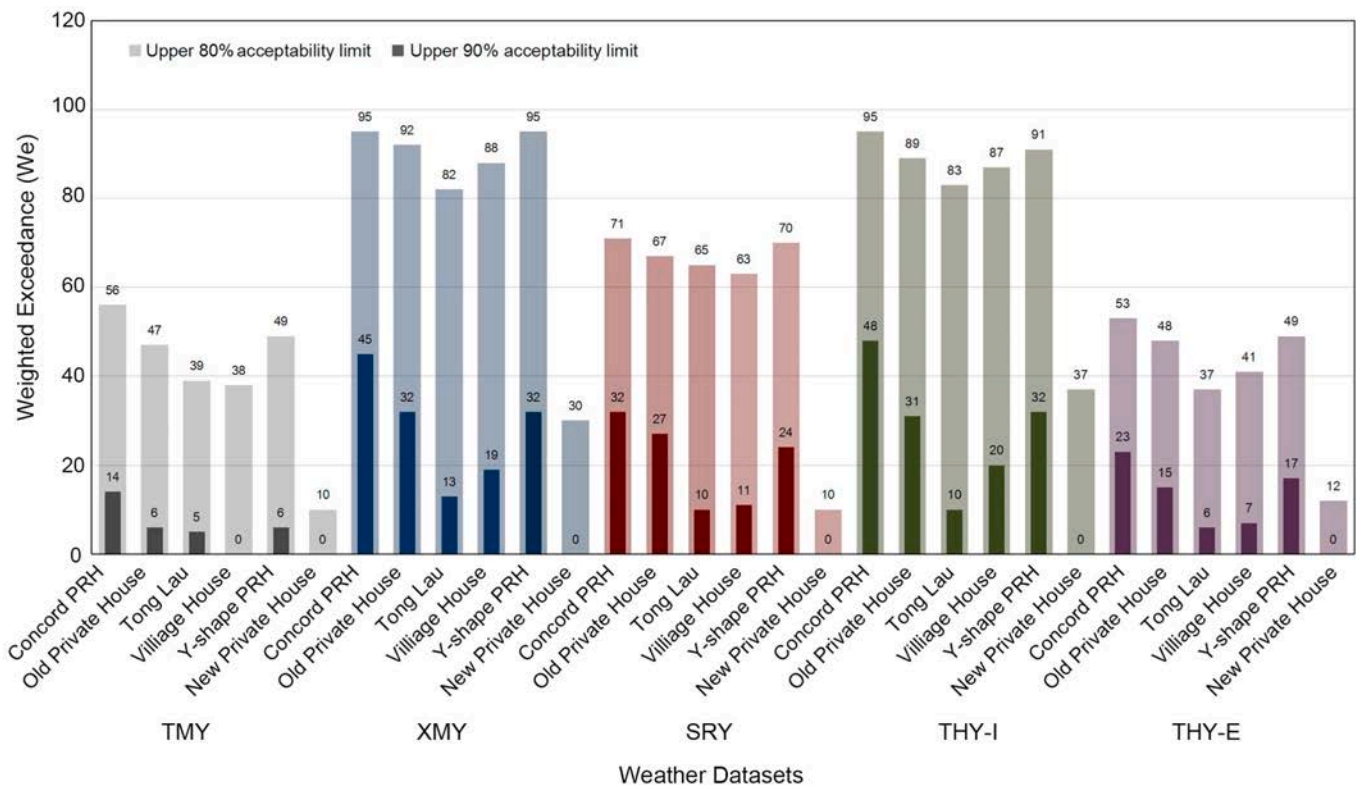
of year in THYs is based on the year with the highest or longest indoor heat event. This study confirms the suitability of the THY-I and THY-E for the assessment of the most extreme overheating risks. On the contrary, the SRY does not fully represent the most extreme overheating risks at nighttime which is critical for the health impacts, such as higher mortality risk [41], and passive survivability of residential buildings in subtropical cities. It is therefore necessary to further incorporate the sorting of daily minimum temperature in the SRY adjustment to better reflect nighttime situations in subtropical climates.

Additionally, different rooms with different shading configurations could considerably affect the applicability of the THY-I and XMY. For example, the highest daytime HI in Tong Lau and Village House was not found when using the THY-I, as shown in Table 6. This is because the living rooms in Tong Lau and Village House are fairly shaded by the other rooms, balconies, or neighboring buildings, and thus are not exposed to direct solar radiation during the daytime, as shown in Fig. 3. Therefore, using the THY-I with a higher solar radiation may not cause more heat stress for well-shaded rooms than using the other weather datasets like the XMY (refer to Fig. A1). As well-shaded buildings are common in a high-density urban setting, the weather data with a higher solar radiation may not provide the most representative conditions for overheating risk assessment in the subtropical high-density cities. Thus, it is plausible to suggest that overheating risk assessment of different buildings in such high-density settings should consider the combination of different extreme weather datasets, for instance, the XMY and the THYs, instead of using only one weather file.

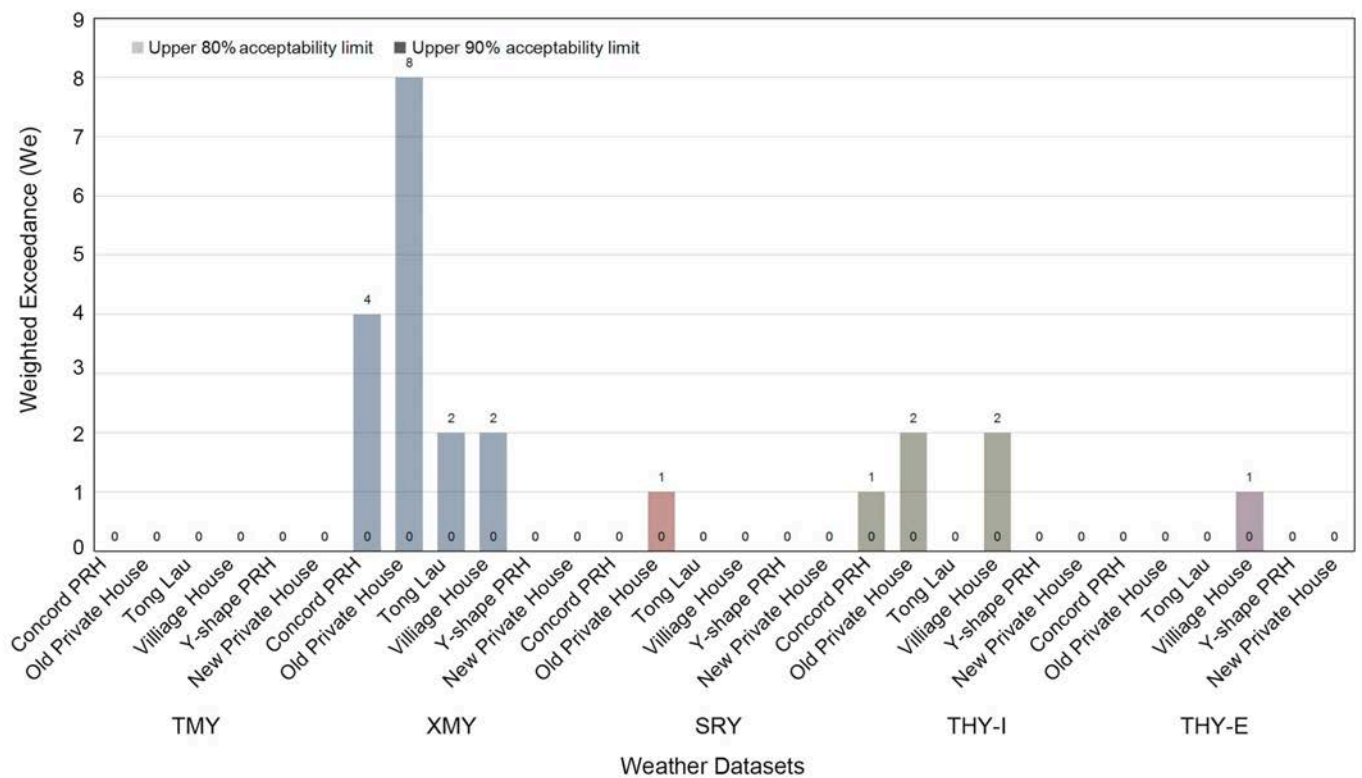
4.2. Performance comparison between different residential archetypes

With respect to the thermal performance comparison among the six archetypes, the indoor average daily range versus average temperature of each archetype are plotted for the different weather conditions in Fig. 11. During summer, the indoor average temperatures in all archetypes were higher than the outdoor average temperature, whereas the indoor average daily temperature ranges were all smaller than those outdoors. This implies that all archetypes release less heat to the outdoor environment at night than the amount absorbed and stored in the buildings during the day. However, the diurnal extreme could be reduced depending on the thermal mass of the building envelope and shading components. This is because the mass of a building provides the thermal capacitance to have inertia against temperature fluctuations and shading components help minimize the solar heat gain to the building envelopes. Among these archetypes, a remarkable trend is that indoor average temperatures for the New Private House showed the smallest difference with outdoor average temperatures, and its average daily range of temperature inside was the lowest, which further implies that the New Private House has the best thermal performance among these archetypes. This can be mainly attributed to the external tinted glazing with low-e coating and balconies with around 1 m projection which has the same function with external shading overhangs, as shown in Table 3 and Fig. 3. Additionally, the living room in the New Private House has a higher WWR and a larger openable window area, which means it can fully utilize the cooling effect of nocturnal natural ventilation and considerably reduce the daytime solar heat gain through the windows.

By contrast, the vulnerability of public housing under different extreme weather conditions was constantly found in the two PRH buildings which showed the largest indoor average temperatures and diurnal temperature extremes. Window glazing with a higher Solar Heat Gain Coefficient and poor external shading designs are mainly responsible for such poor thermal performance in the PRH buildings, as the

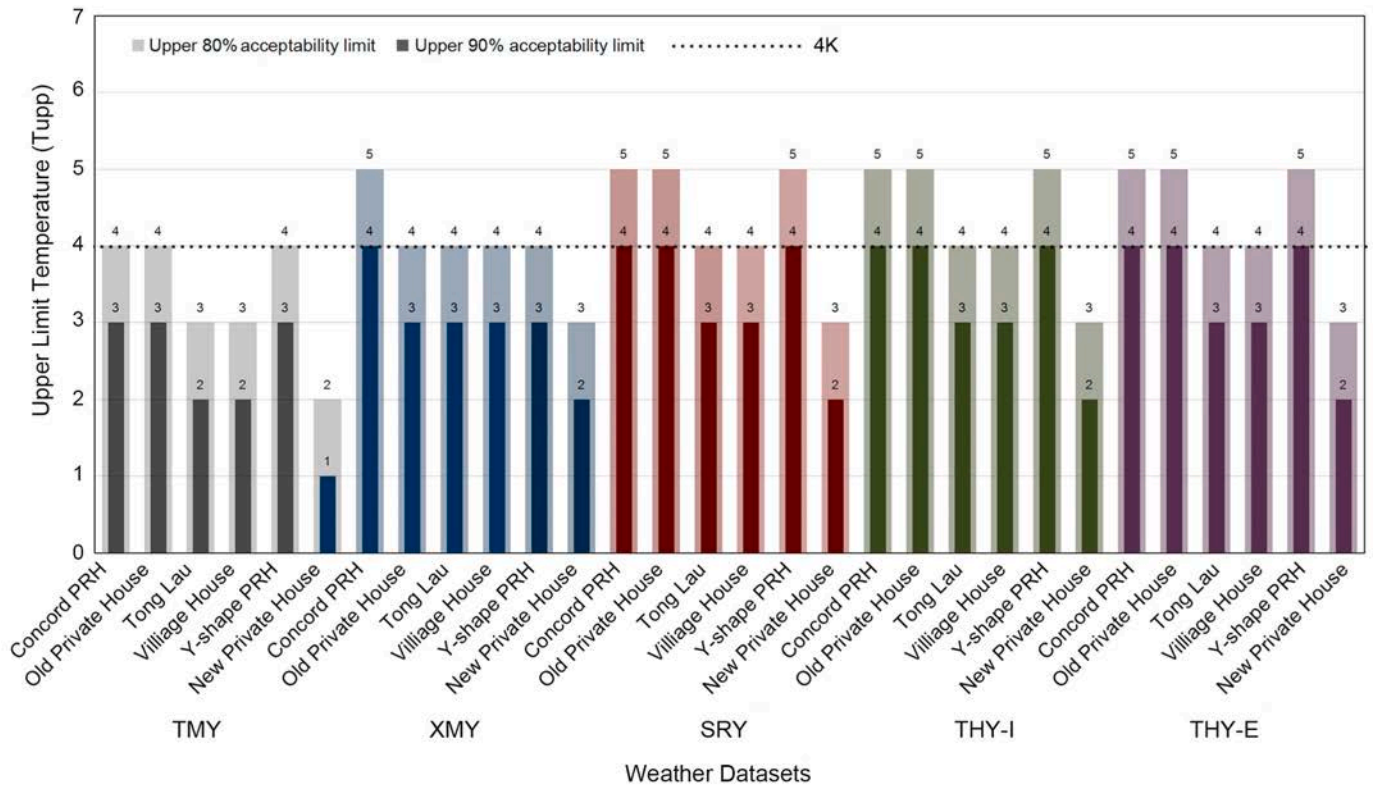


(a)

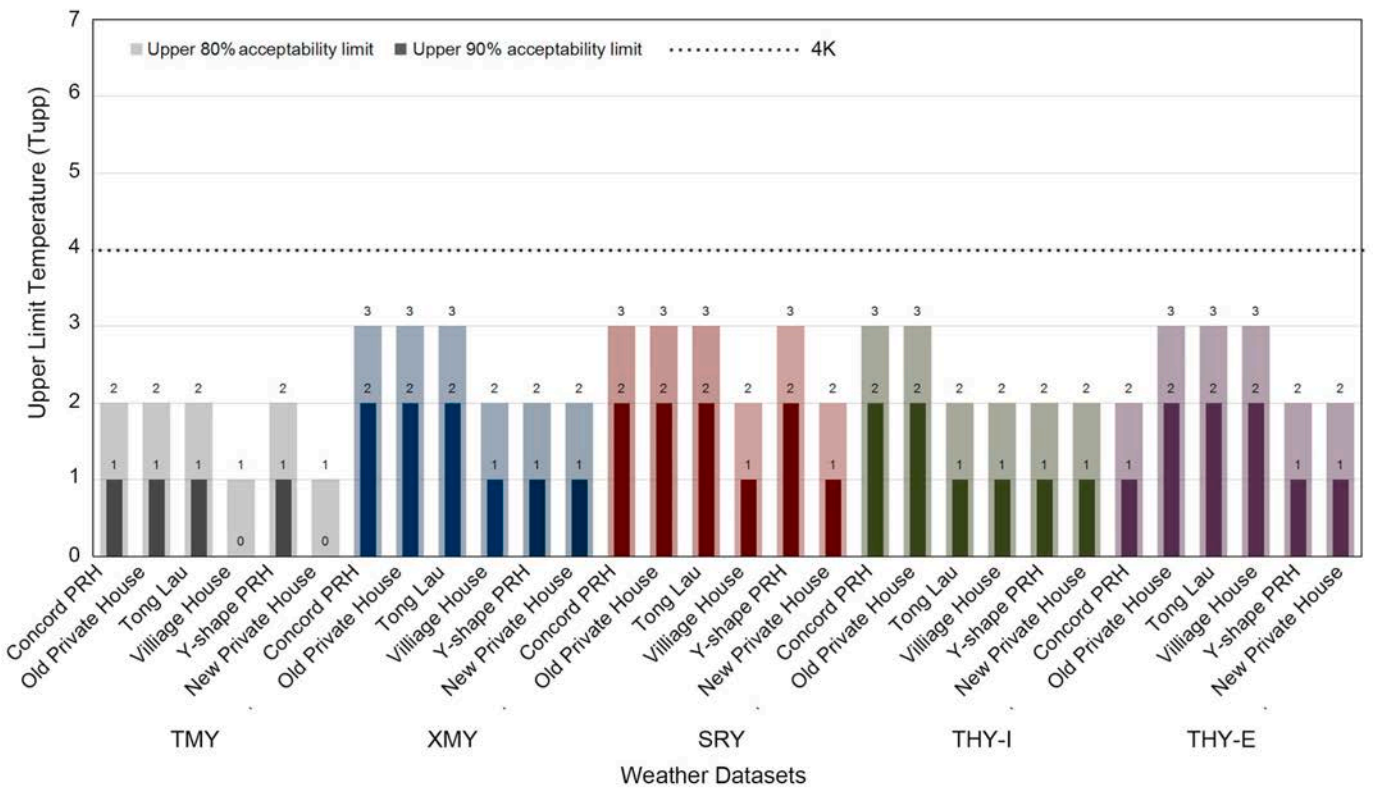


(b)

Fig. 9. The days with Weighted Exceedance (We) more than 6 for different archetypes under different weather conditions (a) living rooms (b) bedrooms.



(a)



(b)

Fig. 10. The upper limit temperature for different archetypes under different weather conditions (a) daytime (b) nighttime.

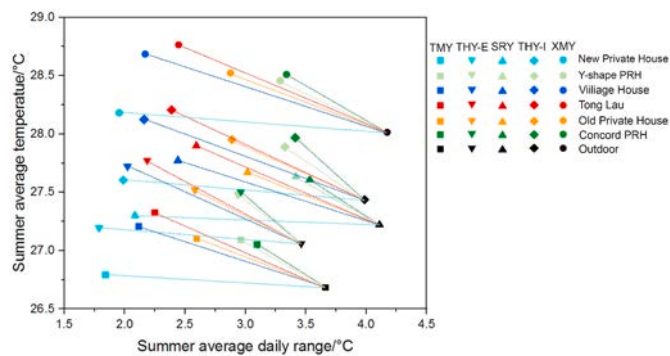


Fig. 11. The relationship between summer average daily range and average temperature in different archetypes and outdoors under different weather conditions.

solar heat gain into a building through windows is deemed more important for building performance in Hong Kong compared with wall insulation [71]. Therefore, to be more adaptive to the changing climate, the design of new PRH buildings or retrofit of existing ones should focus on how to avoid solar heat gain in the daytime, such as designing the balcony for living rooms or bedrooms facing west or east, retrofitting existing glazing with the tinted one with low-e coating, adding external shading devices with longer projection, and simultaneously increasing window openable areas to utilize to best advantage the nocturnal natural ventilation. Moreover, it is observed that the PRH buildings and Tong Lau, which accommodate most of the elderly, physically disabled or financially less capable people, are exposed to higher overheating risks. This reflects a potential correlation between overheating risks and socioeconomic inequity issues for residents living in these buildings. Special attention and actions should thus be given to these vulnerable people and in improving the resilience of PRH buildings and Tong Lau to prolonged overheating conditions.

4.3. Limitations and future works

Different methods to construct extreme weather data are compared in the subtropical high-density Hong Kong residential buildings. Since different meteorological variables may have a different influence on the building thermal performance in a different climate zone, the applicability of different extreme weather datasets should be tested in other climate zones and for other archetypes in the future to demonstrate the validity of and consistency with the findings of this study. As the key aim of this work is to compare the applicability of different weather datasets using the same baseline of 1997–2014, the warmest years experienced in recent years have not been considered in the extreme weather dataset construction. Although the weather datasets only focus on methods based on the historical recorded data, the results can imply the appropriate extreme design weather datasets to provide more robust weather conditions for building thermal simulations if hourly weather data for the more recent years or the future are available.

It should also be noted that the calibration of different models is based on monitoring of typical summer days instead of extreme conditions due to the limited access of these occupied buildings and practical difficulties for a long-term monitoring campaign. It is possible that the

calibrated models do not perform as well under extreme conditions. The results of overheating assessments can also be affected by the assumed occupant behaviour, occupancy, and equipment operation schedule in the modelling. Moreover, it is noteworthy that even if the adaptive thermal comfort model and static thresholds can be used to quantify the overheating risks, a controversy exists on the suitability of applying adaptive models in bedrooms, where occupants have limited adaptive opportunity during nighttime, and the application of evolved thresholds for assessing buildings in use [72]. Additionally, the influence of the urban microclimate conditions around these high-rise buildings has not been taken into account in this study due to the limitations of BPS tools, but the weather data are collected from the HKO Headquarters weather station, which is located in a densely developed station in urban centre Tsim Sha Tsui, Hong Kong. In future works, the urban scale overheating risks could be explored since the building parameters of Hong Kong residential archetypes has been validated and well documented in this study.

5. Conclusion

This comparative study investigated the applicability of four approaches to develop extreme weather datasets for assessing overheating risks during hot and humid summers. After the calibration of building simulation models, overheating risks in six residential archetypes in subtropical Hong Kong under different extreme weather conditions were quantified by static extreme event thresholds and the adaptive TM52 approach. According to the results, different weather datasets have their unique characteristics and limitations for the evaluation of overheating risks in these residential buildings. Overall, the THY-I can be used to identify the most severe HI and He in the daytime, and the THY-E to identify the longest daytime L in most of the modeled archetypes, while the most severe nighttime HI and He can be captured when using the XMY. However, it was found that using the SRY is not suitable for investigating the overheating risks during nighttime and, compared to the XMY, using the THY-I may fail to evaluate the maximum HI of well-shaded buildings. Furthermore, the thermal performance of several typical high-density building types was compared in different extreme climate conditions. The building type with a long projection balcony and a bigger openable window with low-e coating consistently had a better performance than the other building types in different extreme climatic conditions. These results underline the importance of considering the appropriate overheating criteria and extreme weather datasets to ensure robust assessments of passive survivability of residential buildings and the possibility of designing climate resilient buildings to mitigate extreme weather conditions.

Declaration of competing interest

The authors declare that they have no known competing financial interests or personal relationships that could have appeared to influence the work reported in this paper.

Acknowledgement

This work is fully supported by the Vice-Chancellor's Discretionary Fund of the Chinese University of Hong Kong and the Research Impact Fund (Ref: R4046-18F) of Research Grant Council, Hong Kong.

Appendix A

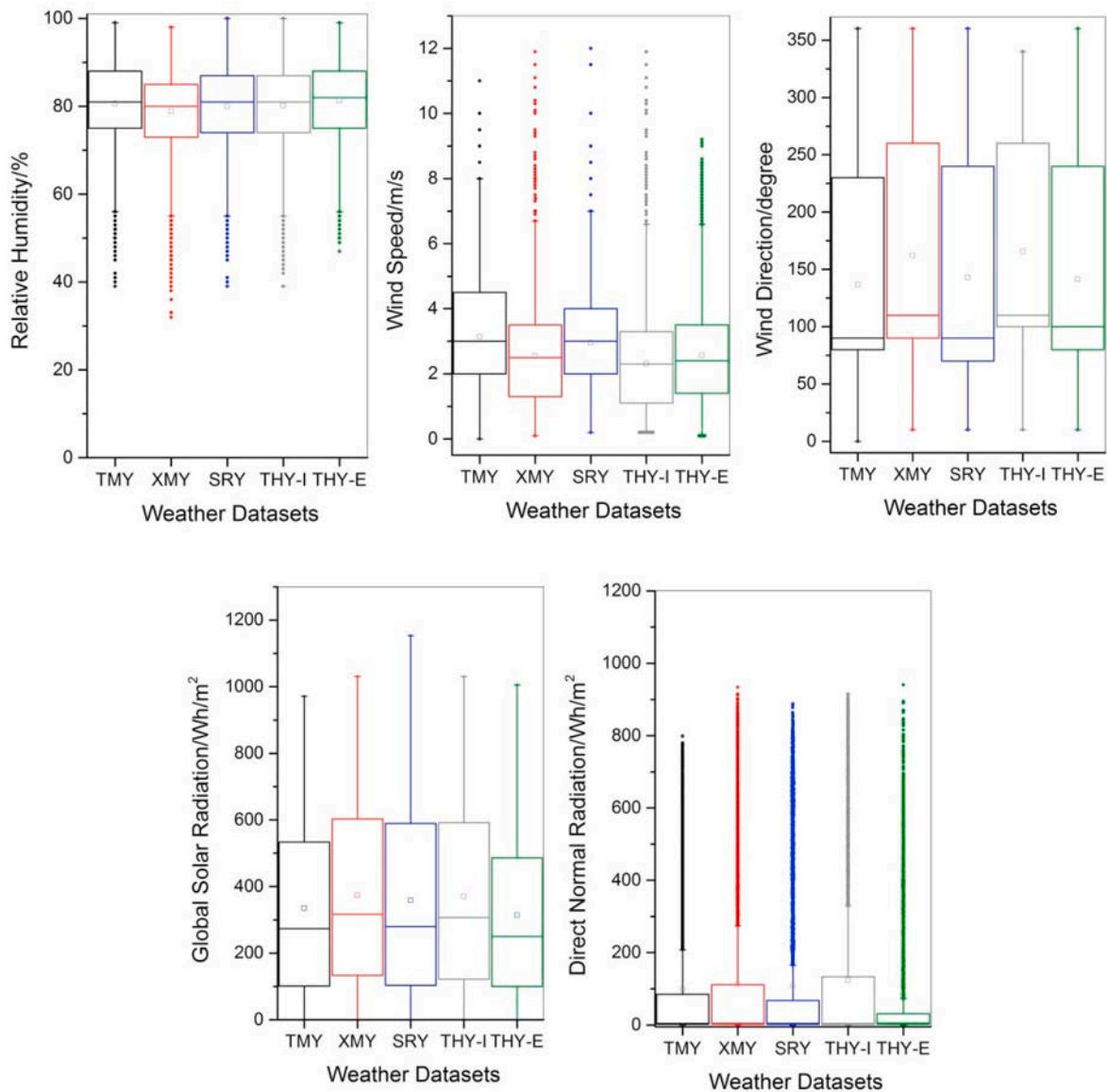


Fig. A1. Boxplots of different meteorological variables under different weather datasets.

Table A1

The metadata of measurement conditions and calibrated building physical parameters of different residential archetypes.

Measurement conditions and building characteristics	Concord PRH	Y-Shape Trident PRH	Old private housing	New private housing	Tong Lau	Village/Individual house
Sky conditions during measurement period	–	Partially cloudy	Clear sky	Clear sky	Partially cloudy	Overcast sky
Test floor location/floors of the whole building	–	18/34	8/9	9/40	4/6	2/3
Occupant activity	–	Unoccupied	Unoccupied	18:00PM-08:00AM	18:00PM(22:00PM)-08:00AM(10:00AM)*	18:00PM(22:00PM)-08:00AM(09:00AM)*
Floor height (m)	2.75	2.70	2.90	2.80	2.70	2.60
Total occupied floor area (m ²)	325.1	920.6	267.5	412.8	124.7	58.4
Window openable area ratio	0.50	0.50	0.60	0.65	0.60	0.85
Window to external wall ratio	0.15	0.31	0.18	0.28	0.22	0.23
U-value of external walls (W/(m ² K))	2.75	3.33	3.30	2.05	3.85	3.30
U-value of floor slabs (W/(m ² K))	2.48	2.48	2.50	2.50	2.75	2.75
U-value of glazing (W/(m ² K))	5.75	5.75	5.75	5.00	5.95	5.75
Solar heat gain coefficient of glazing	0.60	0.60	0.60	0.35	0.85	0.60
External wall solar absorptance	0.58	0.58	0.35	0.65	0.50	0.40
Air flow coefficient of external windows cracks (kg s ⁻¹ m ⁻¹)	0.0018	0.0018	0.0014	0.0010	0.0030	0.0030

Note: means the measurement is not conducted in this building type.

*Means the occupant schedule could be alternative during the measured period.

Table A2

Building occupancy and operation schedule (habitable area).

Hour	Occupancy (Weekdays)	Occupancy (Weekends)	Equipment (Mon-Sun)	Lighting (Mon-Sun)
1	1	1	0.2	0
2	1	1	0.2	0
3	1	1	0.2	0
4	1	1	0.2	0
5	1	1	0.2	0
6	1	1	0.2	0
7	1	1	0.37	0.3
8	0.7	0.9	0.54	0.5
9	0.4	0.7	0.54	0.3
10	0.3	0.6	0.54	0
11	0.3	0.5	0.54	0
12	0.2	0.4	0.54	0
13	0.2	0.3	0.54	0
14	0.2	0.3	0.63	0.5
15	0.2	0.3	0.43	0
16	0.3	0.3	0.43	0
17	0.3	0.4	0.43	0
18	0.4	0.4	0.43	0
19	0.6	0.5	0.43	0.5
20	0.7	0.6	1	1
21	0.8	0.7	1	1
22	0.9	0.8	1	1
23	0.9	0.9	1	1
24	1	1	1	0.5

References

- [1] J. Rogelj, M. Den Elzen, N. Höhne, T. Fransen, H. Fekete, H. Winkler, R. Schaeffer, F. Sha, K. Riahi, M. Meinshausen, Paris Agreement climate proposals need a boost to keep warming well below 2 °C, *Nature* (2016), <https://doi.org/10.1038/nature18307>.
- [2] Intergovernmental Panel on Climate Change, Climate Change 2014 Mitigation of Climate Change. <https://doi.org/10.1017/cbo9781107415416>, 2014.
- [3] N.E. Klepeis, W.C. Nelson, W.R. Ott, J.P. Robinson, A.M. Tsang, P. Switzer, J. V. Behar, S.C. Hern, W.H. Engelmann, The National Human Activity Pattern Survey (NHAPS): a resource for assessing exposure to environmental pollutants, *J. Expo. Anal. Environ. Epidemiol.* (2001), <https://doi.org/10.1038/sj.jea.7500165>.
- [4] H.W. Samuelson, A. Baniassadi, P. Izaga Gonzalez, Beyond energy savings: investigating the co-benefits of heat resilient architecture, *Energy* (2020), <https://doi.org/10.1016/j.energy.2020.117886>.
- [5] A. Baniassadi, D.J. Sailor, E. Scott Krayenhoff, A.M. Broadbent, M. Georgescu, Passive survivability of buildings under changing urban climates across eight US cities, *Environ. Res. Lett.* (2019), <https://doi.org/10.1088/1748-9326/ab28ba>.
- [6] H. Samuelson, S. Claussnitzer, A. Goyal, Y. Chen, A. Romo-Castillo, Parametric energy simulation in early design: high-rise residential buildings in urban contexts, *Build. Environ.* (2016), <https://doi.org/10.1016/j.buildenv.2016.02.018>.
- [7] C. Liu, T. Kershaw, D. Fosas, A.P. Ramallo Gonzalez, S. Natarajan, D.A. Coley, High resolution mapping of overheating and mortality risk, *Build. Environ.* (2017), <https://doi.org/10.1016/j.buildenv.2017.05.028>.
- [8] Z. Zhai, Facial mask: a necessity to beat COVID-19, *Build. Environ.* (2020), <https://doi.org/10.1016/j.buildenv.2020.106827>.
- [9] J. Ren, Y. Wang, Q. Liu, Y. Liu, Numerical study of three ventilation strategies in a prefabricated COVID-19 inpatient ward, *Build. Environ.* (2020), <https://doi.org/10.1016/j.buildenv.2020.107467>.
- [10] A.T.D. Perera, V.M. Nik, D. Chen, J.L. Scartezzini, T. Hong, Quantifying the impacts of climate change and extreme climate events on energy systems, *Nat. Energy.* (2020), <https://doi.org/10.1038/s41560-020-0558-0>.
- [11] J. Taylor, M. Davies, A. Mavrogianni, Z. Chalabi, P. Biddulph, E. Oikonomou, P. Das, B. Jones, The relative importance of input weather data for indoor overheating risk assessment in dwellings, *Build. Environ.* (2014), <https://doi.org/10.1016/j.buildenv.2014.03.010>.
- [12] D.H.W. Li, L. Yang, J.C. Lam, Impact of climate change on energy use in the built environment in different climate zones - a review, *Energy* (2012), <https://doi.org/10.1016/j.energy.2012.03.044>.
- [13] V. Tink, S. Porritt, D. Allinson, D. Loveday, Measuring and mitigating overheating risk in solid wall dwellings retrofitted with internal wall insulation, *Build. Environ.* (2018), <https://doi.org/10.1016/j.buildenv.2018.05.062>.
- [14] J. Morey, A. Bezaee, A. Wright, An investigation into overheating in social housing dwellings in central England, *Build. Environ.* (2020), <https://doi.org/10.1016/j.buildenv.2020.106814>.
- [15] S.M. Tabatabaei Sameni, M. Gaterell, A. Montazami, A. Ahmed, Overheating investigation in UK social housing flats built to the Passivhaus standard, *Build. Environ.* (2015), <https://doi.org/10.1016/j.buildenv.2015.03.030>.
- [16] T. van Hooff, B. Blocken, H.J.P. Timmermans, J.L.M. Hensen, Analysis of the predicted effect of passive climate adaptation measures on energy demand for cooling and heating in a residential building, *Energy* (2016), <https://doi.org/10.1016/j.energy.2015.11.036>.
- [17] M. Hamdy, S. Carlucci, P.J. Hoes, J.L.M. Hensen, The impact of climate change on the overheating risk in dwellings—a Dutch case study, *Build. Environ.* (2017), <https://doi.org/10.1016/j.buildenv.2017.06.031>.
- [18] A. Dodo, L. Gustavsson, Energy use and overheating risk of Swedish multi-storey residential buildings under different climate scenarios, *Energy* (2016), <https://doi.org/10.1016/j.energy.2015.12.086>.
- [19] R.L. Hwang, T.P. Lin, F.Y. Lin, Evaluation and mapping of building overheating risk and air conditioning use due to the urban heat island effect, *J. Build. Eng.* (2020), <https://doi.org/10.1016/j.jobe.2020.101726>.
- [20] J.C. Gamero-Salinas, A. Monge-Barrio, A. Sánchez-Ostiz, Overheating risk assessment of different dwellings during the hottest season of a warm tropical climate, *Build. Environ.* (2020), <https://doi.org/10.1016/j.buildenv.2020.106664>.
- [21] M. Roth, Review of urban climate research in (sub)tropical regions, *Int. J. Climatol.* (2007), <https://doi.org/10.1002/joc.1591>.
- [22] Census, Statistics Department, Hong Kong Poverty Situation Report 2019, Hong Kong, 2019 accessed, <https://www.censtatd.gov.hk/hkstat/>. (Accessed 18 May 2020).
- [23] H. Chen, W.L. Lee, Combined Space Cooling and Water Heating System for Hong Kong Residences, *Energy Build.* (2010), <https://doi.org/10.1016/j.enbuild.2009.08.020>.
- [24] Y. Wu, H. Liu, B. Li, R. Kosonen, D. Kong, S. Zhou, R. Yao, Thermal adaptation of the elderly during summer in a hot humid area: psychological, behavioral, and physiological responses, *Energy Build.* (2019), <https://doi.org/10.1016/j.enbuild.2019.109450>.
- [25] D. Wang, K.K.L. Lau, C. Ren, W.B. Goggins, Y. Shi, H.C. Ho, T.C. Lee, L.S. Lee, J. Woo, E. Ng, The impact of extremely hot weather events on all-cause mortality in a highly urbanized and densely populated subtropical city: a 10-year time-series study (2006–2015), *Sci. Total Environ.* (2019), <https://doi.org/10.1016/j.scitotenv.2019.07.039>.
- [26] H. Samuelson, A. Baniassadi, A. Lin, P. Izaga Gonzalez, T. Brawley, T. Narula, Housing as a critical determinant of heat vulnerability and health, *Sci. Total Environ.* (2020), <https://doi.org/10.1016/j.scitotenv.2020.137296>.
- [27] A.L.S. Chan, T.T. Chow, S.K.F. Fong, J.Z. Lin, Generation of a typical meteorological year for Hong Kong, *Energy Convers. Manag.* (2006), <https://doi.org/10.1016/j.enconman.2005.02.010>.
- [28] ASHRAE, Weather Year for Energy Calculations, ASHRAE, Atlanta, 1985.
- [29] NCD, Test Reference Year, in Tape Reference Manual, TD-9706. Asheville, U.S.: National Climate Data Center, U.S. Dept. of Commerce, 1976.
- [30] G.J. Levermore, J.B. Parkinson, Analyses and algorithms for new test reference years and design summer years for the UK, *Build. Serv. Eng. Technol.* (2006), <https://doi.org/10.1177/0143624406071037>.
- [31] R. Watkins, G.J. Levermore, J.B. Parkinson, The design reference year - a new approach to testing a building in more extreme weather using UKCP09 projections, *Build. Serv. Eng. Technol.* (2013), <https://doi.org/10.1177/0143624411431170>.

- [32] M.F. Jentsch, M.E. Eames, G.J. Levermore, Generating near-extreme Summer Reference Years for building performance simulation, *Build. Serv. Eng. Technol.* (2015), <https://doi.org/10.1177/0143624415587476>.
- [33] D.B. Crawley, L.K. Lawrie, Rethinking the tmy: is the "typical" meteorological year best for building performance simulation?, in: 14th Int. Conf. IBPSA - Build. Simul. 2015, BS 2015, Conf. Proc., 2015.
- [34] S. Guo, D. Yan, T. Hong, C. Xiao, Y. Cui, A novel approach for selecting typical hot-year (THY) weather data, *Appl. Energy* (2019), <https://doi.org/10.1016/j.apenergy.2019.03.065>.
- [35] P. Narowski, M. Janicki, D. Heim, Comparison of untypical meteorological years (umy) and their influence on building energy performance simulations, in: *Proc. BS 2013 13th Conf. Int. Build. Perform. Simul. Assoc.*, 2013.
- [36] V.M. Nik, Making energy simulation easier for future climate - synthesizing typical and extreme weather data sets out of regional climate models (RCMs), *Appl. Energy* (2016), <https://doi.org/10.1016/j.apenergy.2016.05.107>.
- [37] S. Liu, W.J. Chung, D. Coley, Creation of future hot event years for assessing building resilience against future deadly heatwaves, in: *Proceedings of the 16th IBPSA Conference, Rome, Italy, Sept. 2-4, 2019*, <https://doi.org/10.26868/25222708.2019.210527>.
- [38] Y. Cui, D. Yan, T. Hong, C. Xiao, X. Luo, Q. Zhang, Comparison of typical year and multiyear building simulations using a 55-year actual weather data set from China, *Appl. Energy* (2017), <https://doi.org/10.1016/j.apenergy.2017.03.113>.
- [39] CIBSE, *The limits of thermal comfort : avoiding overheating in European buildings, 2013. CIBSE Tm52*.
- [40] C.S.C. Cheung, M.A. Hart, Climate change and thermal comfort in Hong Kong, *Int. J. Biometeorol.* (2014), <https://doi.org/10.1007/s00484-012-0608-9>.
- [41] K.K.L. Lau, E.Y.Y. Ng, P.W. Chan, J.C.K. Ho, Near-extreme summer meteorological data set for sub-tropical climates, *Build. Serv. Eng. Technol.* (2017), <https://doi.org/10.1177/0143624416675390>.
- [42] S. Guo, D. Yan, C. Gui, The typical hot year and typical cold year for modeling extreme events impacts on indoor environment: a generation method and case Study, *Build. Simul.* (2020), <https://doi.org/10.1007/s12273-020-0617-2>.
- [43] T.E. Morakinyo, C. Ren, Y. Shi, K.K.L. Lau, H.W. Tong, C.W. Choy, E. Ng, Estimates of the impact of extreme heat events on cooling energy demand in Hong Kong, *Renew. Energy* (2019), <https://doi.org/10.1016/j.renene.2019.04.077>.
- [44] H.C. Ho, K.K.L. Lau, C. Ren, E. Ng, Characterizing prolonged heat effects on mortality in a sub-tropical high-density city, *Hong Kong, Int. J. Biometeorol.* (2017), <https://doi.org/10.1007/s00484-017-1383-4>.
- [45] Hong Kong, Observatory, *Statistics of Special Weather Events: Number of Hot Nights, 2020*. https://www.hko.gov.hk/en/cis/statistic/hngtday_statistic.htm. (Accessed 2 February 2021). accessed.
- [46] Y.T. Kwok, A.K.L. Lai, K.K.L. Lau, P.W. Chan, Y. Lavafpour, J.C.K. Ho, E.Y.Y. Ng, Thermal comfort and energy performance of public rental housing under typical and near-extreme weather conditions in Hong Kong, *Energy Build* (2017), <https://doi.org/10.1016/j.enbuild.2017.09.067>.
- [47] I. Ballarini, S.P. Corgnati, V. Corrado, Use of reference buildings to assess the energy saving potentials of the residential building stock: the experience of TABULA Project, *Energy Policy* (2014), <https://doi.org/10.1016/j.enpol.2014.01.027>.
- [48] BEAM, *BEAM Plus New Buildings Version 1.2*, HKGBC and BEAM Society Limited, 2012.
- [49] H. Chen, W.L. Lee, F.W.H. Yik, Applying water cooled air conditioners in residential buildings in Hong Kong, *Energy Convers. Manag.* (2008), <https://doi.org/10.1016/j.enconman.2007.12.024>.
- [50] Hong Kong Housing Authority, *HKHA Annual Report 2017/2018, 2018*.
- [51] Hong Kong Housing Authority, *Housing Authority Public Housing Portfolio, 2018*.
- [52] V. Masson, W. Heldens, E. Bocher, M. Bonhomme, B. Bucher, C. Burmeister, C. de Munck, T. Esch, J. Hidalgo, F. Kanani-Sühring, Y.T. Kwok, A. Lemonsu, J.P. Lévy, B. Maronga, D. Pavlik, G. Petit, L. See, R. Schoetter, N. Tornay, A. Votsis, J. Zeidler, City-descriptive input data for urban climate models: model requirements, data sources and challenges, *Urban Clim* (2020), <https://doi.org/10.1016/j.uclim.2019.100536>.
- [53] Y.T. Kwok, C. De Munck, R. Schoetter, C. Ren, K.K.L. Lau, Refined dataset to describe the complex urban environment of Hong Kong for urban climate modelling studies at the mesoscale, *Theor. Appl. Climatol.* (2020), <https://doi.org/10.1007/s00704-020-03298-x>.
- [54] Y.T. Kwok, R. Schoetter, V. Masson, Defining building archetypes for urban climate simulations of the complex high-density environment in Hong Kong, in: *PLEA 2018 - Smart Heal. Within Two-Degree Limit Proc. 34th Int. Conf. Passiv. Low Energy Archit.*, 2018.
- [55] R. Schoetter, Y.T. Kwok, C. de Munck, K.K.L. Lau, W.K. Wong, V. Masson, Multi-layer coupling between SURFEX-TEB-v9.0 and Meso-NH-v5.3 for modelling the urban climate of high-rise cities, *Geosci. Model Dev. (GMD)* (2020), <https://doi.org/10.5194/gmd-13-5609-2020>.
- [56] Housing Department, *Standard Block Typical Floor Plans, Hong Kong, 2019* accessed, <https://www.housingauthority.gov.hk/en/global-elements/estate-locator/standard-block-typical-floor-plans/>. (Accessed 11 April 2020).
- [57] Electrical, Mechanical Services Department, *Code of Practice for Energy Efficiency of Building Services Installation*. https://www.emsd.gov.hk/beeo/en/pee/BEC_2018.pdf, 2018. (Accessed 23 January 2020) accessed.
- [58] S.C. Snyder, I. Maor, *Calibrated building energy simulation in practice: issues, approaches, and case study example*, *Build. Eng.* (2015).
- [59] A. O' Donovan, P.D. O' Sullivan, M.D. Murphy, Predicting air temperatures in a naturally ventilated nearly zero energy building: calibration, validation, analysis and approaches, *Appl. Energy* (2019), <https://doi.org/10.1016/j.apenergy.2019.04.082>.
- [60] ANSI/ASHRAE, *ASHRAE Guideline 14-2002 Measurement of Energy and Demand Savings*, Ashrae, 2002.
- [61] D. Chakraborty, H. Elzarka, Performance testing of energy models: are we using the right statistical metrics? *J. Build. Perform. Simul.* (2018) <https://doi.org/10.1080/19401493.2017.1387607>.
- [62] P. Xue, C.M. Mak, Y. Huang, Quantification of luminous comfort with dynamic daylight statistical metrics in residential buildings, *Energy Build* (2016), <https://doi.org/10.1016/j.enbuild.2016.02.026>.
- [63] K.F. Fong, C.K. Lee, Investigation of separate or integrated provision of solar cooling and heating for use in typical low-rise residential building in subtropical Hong Kong, *Renew. Energy* (2015), <https://doi.org/10.1016/j.renene.2014.10.069>.
- [64] M. Bojić, F. Yik, Application of advanced glazing to high-rise residential buildings in Hong Kong, *Build. Environ.* (2007), <https://doi.org/10.1016/j.buildenv.2005.09.021>.
- [65] F. Nicol, M. Humphreys, Derivation of the adaptive equations for thermal comfort in free-running buildings in European standard EN15251, *Build. Environ.* (2010), <https://doi.org/10.1016/j.buildenv.2008.12.013>.
- [66] A.T. Nguyen, M.K. Singh, S. Reiter, An adaptive thermal comfort model for hot humid South-East Asia, *Build. Environ.* (2012), <https://doi.org/10.1016/j.buildenv.2012.03.021>.
- [67] Y. Zhang, J. Wang, H. Chen, J. Zhang, Q. Meng, Thermal comfort in naturally ventilated buildings in hot-humid area of China, *Build. Environ.* (2010), <https://doi.org/10.1016/j.buildenv.2010.05.024>.
- [68] V. Cheng, E. Ng, Comfort temperatures for naturally ventilated buildings in Hong Kong, *Architect. Sci. Rev.* (2006), <https://doi.org/10.3763/asre.2006.4924>.
- [69] A. Moazami, V.M. Nik, S. Carlucci, S. Geving, Impacts of future weather data typology on building energy performance - investigating long-term patterns of climate change and extreme weather conditions, *Appl. Energy* (2019), <https://doi.org/10.1016/j.apenergy.2019.01.085>.
- [70] D. Virk, M. Eames, *CIBSE Weather Files 2016 Release: Technical Briefing and Testing*, 1. Virk D, Eames M, CIBSE Weather Files 2016 Release Tech. Brief. Testing, 2016.
- [71] S. Liu, Y.T. Kwok, K.K.L. Lau, W. Ouyang, E. Ng, Effectiveness of passive design strategies in responding to future climate change for residential buildings in hot and humid Hong Kong, *Energy Build* (2020), <https://doi.org/10.1016/j.enbuild.2020.110469>.
- [72] K.J. Lomas, S.M. Porritt, Overheating in buildings: lessons from research, *Build. Res. Inf.* (2017), <https://doi.org/10.1080/09613218.2017.1256136>.